Sustainable Structures
ISSN: 2789-3111 (Print); ISSN: 2789-312X (Online)
http://www.sustain-dpl.com/journal/sust
DOI: 10.54113/j.sust.2024.000035

REVIEW ARTICLE

State-of-the-art review on steel-concrete composite walls

Chao-Qun Yu[a], Jing-Zhong Tong[b,*], Si-Ming Zhou[a], Jia-Ming Zhang[a], Jia-Jia Shen[b], Lei Zhang[a], Gen-Shu Tong[a], Qing-Hua Li[a], Shi-Lang Xu[a]

[a]Institute of Advanced Engineering Structures, Zhejiang University, Hangzhou 310058, China.
[b]Exeter Technologies Group (ETG), Department of Engineering, University of Exeter, Exeter EX4 4QF, UK.
[*]Corresponding Author: Jing-Zhong Tong. Email: tongjz@zju.edu.cn.

Abstract: Steel-concrete composite walls, valued for their capacity to combine the strengths of steel and concrete, have become a prevalent construction choice. During the past few decades, the performance of steel-concrete composite walls has been studied by means of structural tests, theoretical analysis, and numerical simulation. Different types of steel-concrete composite walls have been proposed by researchers to satisfy miscellaneous structural requirements. Meanwhile, new forms were continually being developed to further improve the mechanical performance. This review paper examines research conducted over the past few years on these versatile structural elements. The paper categorizes steel-concrete composite walls according to the arrangement of steel plates and concrete, along with the configurations of steel plates. It delves into the unique characteristics of each type and analyzes their performance under various loading conditions, including axial, cyclic, shear, fire, dynamic, impact, and joint loads. Additionally, existing design recommendations for these walls are summarized. To conclude, the paper offers insights into potential future developments in steel-concrete composite wall technology.

Keywords: Steel-concrete composite wall; state-of-the-art review; flat steel plate; corrugated steel plate; multi-celled structure

1 Introduction

Composite structures have become ubiquitous across various engineering disciplines, playing a vital role in modern construction practices [1, 2]. Their exceptional performance stems from the combined action of different materials, each contributing properties that they might not possess individually. Steel-concrete composite structures are the most prevalent example in civil engineering, with their use dating back to the early 20th century, particularly in America, Japan, and Europe [3]. Recent decades have witnessed a surge in the development of various composite systems and components, including composite columns, plates, beams, and walls [4-7].

The shear wall is an important lateral resistance component in structures [8, 9], which are responsible for bearing shear forces and dissipating seismic energy during earthquakes, thereby becoming a significant component in the buildings. With the development of high-rise building systems, the height of the structure continues to increase and the layouts become more complex. This requires a higher performance of shear wall components. As a result, new shear wall structures with excellent performance of seismic resistance and load-bearing capacities are increasingly needed. The reinforced concrete (RC) shear wall and steel plate shear wall (SPSW) are two common forms of the traditional

Received: 24 March 2024; Received in revised form: 9 April 2024; Accepted: 8 May 2024

shear wall. Although the RC structures have good durability performance [10-12], the large wall depth reduces the effective usable area with large self-weight. Therefore, RC shear walls are not appropriate for ultra-high-rise structures. Besides, the RC shear wall is easy to concrete crush under cyclic loads, exhibiting poor ductility. In contrast, the SPSW has good ductility, but its durability and fire resistance are relatively poor. For thick SPSWs, the residual stress and deformation after welding are commonly large, resulting in a great reduction in their mechanical properties. The large consumption of steel and high cost also limit the application of thick SPSWs. For thin SPSWs, the steel plate is easy to buckle under seismic effects. It should be mentioned that thin SPSWs have a large out-of-plane deformation accompanied by noise after buckling. Although these phenomena have little effect on structural safety, they can easily make people feel uncomfortable.

Studies have shown that the steel-concrete composite wall presents significant environmental benefits [13]. The composite wall can effectively combine the advantages of both steel and concrete materials, resulting in a high utilization efficiency of materials and a composite effect greater than the sum of their individual performances. The high durability and longevity of the composite wall minimize the requirement for frequent maintenance and replacement, reducing material waste and resource consumption. Besides, steel is a highly recyclable material, allowing for the potential recovery and reuse of components at the end of the life cycle of the composite wall, promoting a sustainable circular economy. As a result, the steel-concrete composite walls have great load-bearing capacities, high ductility and durability, and excellent environmental friendliness [14, 15]. Due to these advantages, steel-concrete composite walls have gained extensive practical application, as illustrated in Fig. 1.

This paper presents a review of various types of steel-concrete composite walls to provide a clear vision for researchers. Firstly, the steel-concrete composite wall was classified according to the arrangement of steel plates and concrete, along with the configurations of steel plates. Then, research works on the structural behavior of steel-concrete composite walls subjected to different types of loading, e.g. axial compression, lateral loads, cyclic loads, fire resistance, dynamic loads, impact loads, and joint performance, are summarized. The design criteria are analyzed as well and some typical studies are introduced in detail. Finally, based on the review of existing studies, the development trend of steel-concrete composite walls in the future is discussed.

(a) Concrete-encased composite wall (b) Concrete-filled composite wall

Fig. 1. Application of steel-concrete composite walls in practice [16, 17].

2 Classification of steel-concrete composite walls

According to the arrangement of steel plates and concrete as well as the configurations of steel plates, the steel-concrete composite wall can be classified into five groups as shown in Fig. 2, including steel plate reinforced concrete composite wall (SPRCCW), double-skin flat plate composite wall (DFPCW), double-skin corrugated plate composite wall (DCPCW), multi-celled concrete-filled steel tubular wall (MCFSTW) and multi-celled corrugated-plate concrete-filled steel tubular wall (MC-CFSTW).

As described in Fig. 2(a), the SPRCCW consists of a steel plate embedded within reinforced concrete. To strengthen the interaction between steel and concrete, shear connectors are applied, such

as shear studs and steel bars [18]. The presence of the steel plate significantly improves the ductility of the SPRCCW, while maintaining a reduced wall depth for equivalent strength and stiffness [19]. Besides, the concrete restrains the buckling of steel plates, thereby increasing the strength of the wall. The use of external concrete also provides sound and temperature insulation [20].

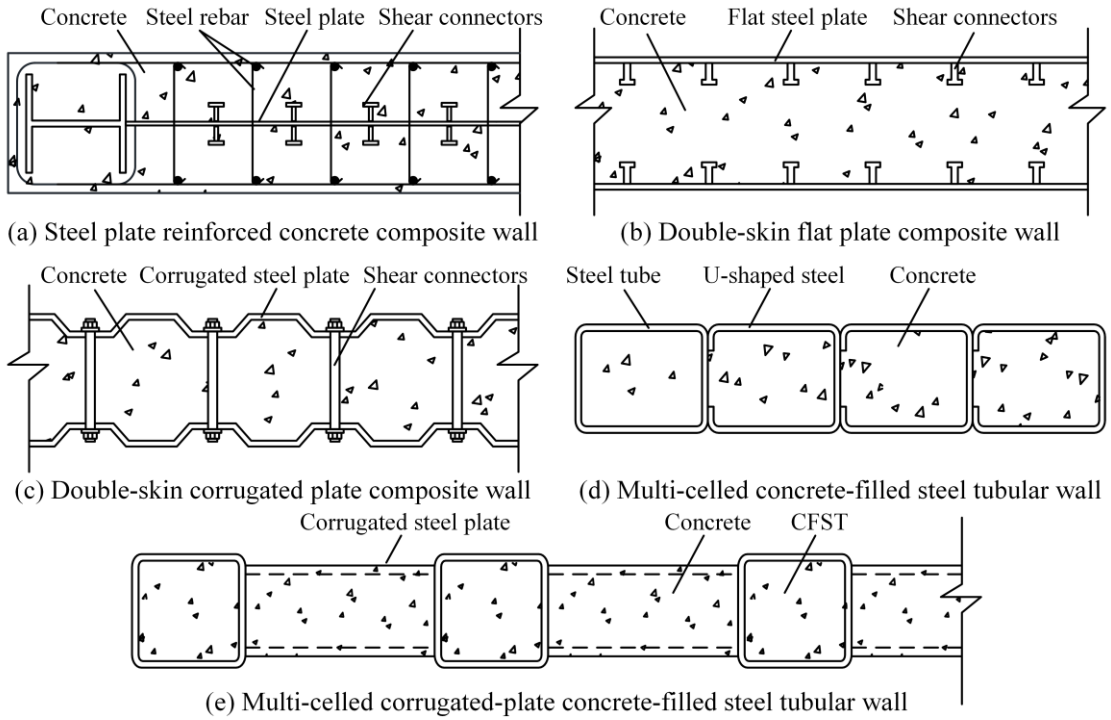

Fig. 2. Different types of steel-concrete composite walls.

However, concrete is easy to crack or even spall under loads, leading to the development of the double-skin composite wall. According to the shape of steel plates, the double-skin composite wall can be divided into DFPCW and DCPCW, as depicted in Fig. 2(b) and (c), respectively. Both DFPCW and DCPCW are composed of two external steel plates filled with concrete, exhibiting good structural performances [21, 22]. On the one hand, the concrete is confined by external steel plates, enhancing its axial compression strength. On the other hand, the concrete restrains the inward deformation of the steel plates, increasing their buckling load capacity [23]. The steel plates can be used as the permanent template of concrete, improving construction efficiency. To ensure the composite action of steel and concrete and prevent local buckling of steel plates, shear connectors are employed [24]. For DFPCWs, dense arrangement of shear connectors to maintain the mechanical properties of the flat steel plates, which imposes higher requirements on the fluidity of the concrete [25]. Simultaneously, it is not conducive to the economic design. Since the bending stiffness is small for the flat steel plate, additional lateral supports may be required to prevent its buckling.

To restrain the local buckling of external steel plates, the corrugated steel plate has been applied in the composite wall [26]. Compared with DFPCWs, the DCPCWs have a better bonding effect between steel plates and concrete, owing to the existence of corrugation. This reduces the demand for shear connectors [27]. Moreover, the bending stiffness of corrugated steel plate about the strong axis is greater than that of flat steel plate with the same thickness by two or three orders of magnitude, which offers stronger confinement for the concrete and meet the rigidity requirements during transportation and installation [28].

As presented in Fig. 2(d), the most widely used MCFSTW consists of a rectangular steel tube and multiple U-shaped steel tubes infilled with concrete [29, 30]. The diaphragm plates in MCFSTWs eliminates the need for shear connectors, which improves construction convenience compared with DFPCWs. Through reasonable design, the steel plate can yield before buckling, ensuring effective interaction between steel and concrete. Since the strength and stiffness of the MCFSTW can be adjusted by the quantity of U-shaped steel tubes, the cross-sectional dimensions of the U-shaped steel tubes are

limited to a few modular sizes in practice, which is beneficial for industrialized construction [31].

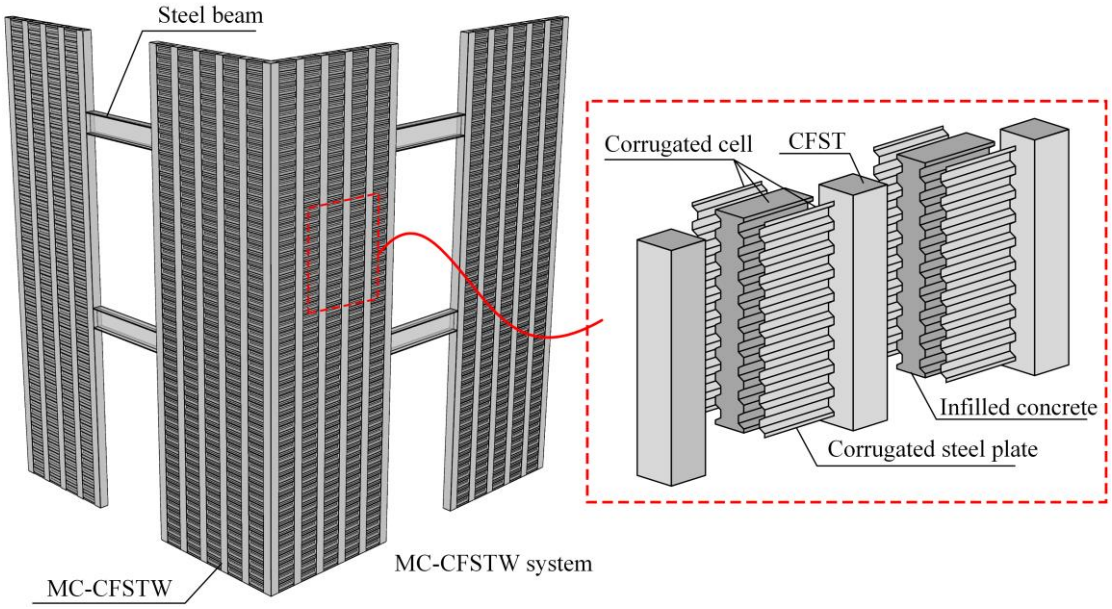

Fig. 3. Diagram of MC-CFSTW.

Table 1. Characteristics of different types of steel-concrete composite walls

Types	Advantages	Disadvantages
SPRCCW	Steel plate without local buckling; High durability and fire resistance	Easy cracking of concrete; Low construction efficiency
DFPCW	Steel plate served as the permanent template; Improving compressive strength of concrete	Easy buckling of steel plates; A large number of connectors
DCPCW	Improving buckling resistance of steel plate; Improving compressive strength of concrete	Limited thickness of corrugated steel plate; Difficulty of welding of corrugated steel plate
MCFSTW	Improving compressive strength of concrete; Without additional connectors	Large steel consumption; Heavy welding workload
MC-CFSTW	Improving compressive strength of concrete; Reducing steel consumption	Difficulty in concrete pouring; High welding requirements

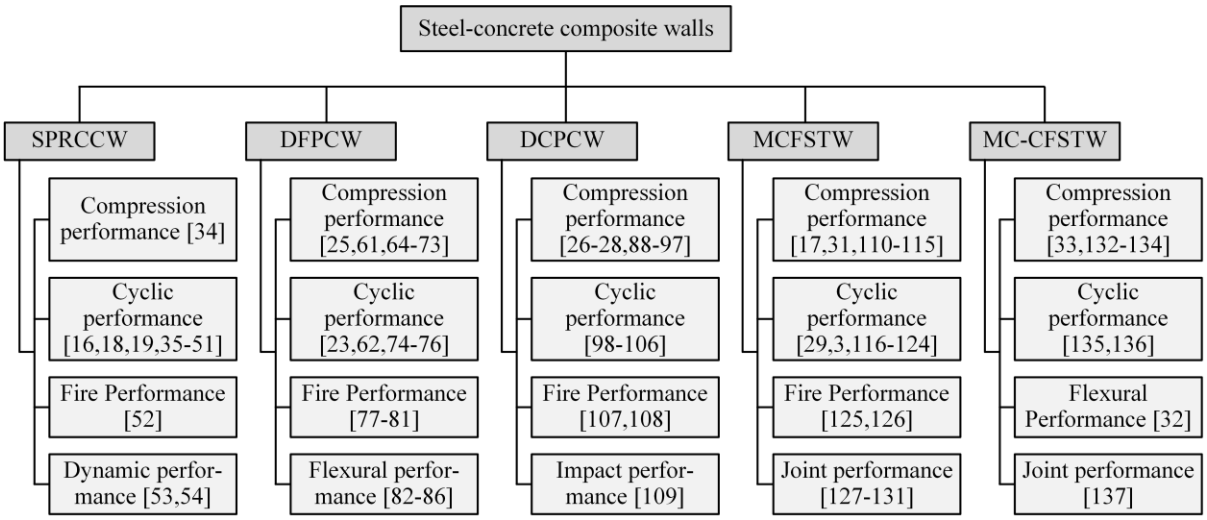

Fig. 4. The research framework.

Though the MCFSTW exhibits high performance in the practical design, the large steel consumption limited its development. As plotted in Fig. 2(e), the MC-CFSTW was proposed by

introducing the corrugated steel plates into multi-celled structures [32]. The MC-CFSTW consists of CFSTs and corrugated cells connected alternately. The diagram of the MC-CFSTW is shown in Fig. 3. Compared to MCFSTWs, U-shaped steel tubes (typically 4 mm in thick) are replaced with corrugated steel plates (typically 1.5 mm in thick), significantly reducing steel consumption. Since the corrugated steel plates are positioned horizontally, the corrugation trough tends to deform inward, providing active confinement on the concrete [33]. The presence of corrugations also reduces the self-weight of the composite wall. However, it also increases the difficulty of concrete pouring and imposes higher welding requirements. Additionally, the ultimate resistance of the MCFSTW relies on the trough section, resulting in underutilization of the material strength at the crest section.

Table 1 summarizes the characteristics of five types of steel-concrete composite walls, and numerous research works have been carried out. As described in **Fig. 4**, research works focused on compression performance, cyclic performance, fire performance, dynamic performance, flexural performance, and joint performance of composite walls.

3 Research on steel plate reinforced concrete composite wall

3.1 Compression performance

Though SPRCCWs were usually designed as lateral resistance members, they were still subjected to axial loads. To investigate their axial behavior, an experimental test was conducted by Hao et al. [34]. Two different shear connectors were involved, including shear studs and vertical stiffening ribs. As described in **Fig. 5**, the concrete near the top end of the wall with shear studs crushed suddenly at the peak load. For specimens with vertical stiffening ribs, the brittle performance improved significantly.

(a) With shear studs (b) With stiffening ribs

Fig. 5. Failure modes of SPRCCW under axial compression [34].

3.2 Cyclic performance

Research works on the SPRCCW mainly focus on its seismic performance. Wang et al. [18] carried out comprehensive tests on 16 specimens of the SPRCCW, revealing that the failure modes varied with the aspect ratio and depth of the wall. Bending failure occurred in the wall with large aspect ratio and small depth, while the wall with small aspect ratio and large depth exhibited bending-shear failure, as presented in Fig. 6. Numerical analyses were conducted by Wang et al. [35] to further study the the seismic performance of the SPRCCW, and the results indicated that increasing steel plate ratio and decreasing axial compressive ratio could enhance the ultimate resistance and deformation capacity of the SPRCCW. Experimental studies on T-shaped SPRCCW under combined axial compression and cyclic lateral loads were conducted by Ke et al. [16]. Compared to I-shaped walls, the T-shaped SPRCCW demonstrated more favorable seismic performance. Ke et al. [19] also proposed a novel type of SPRCCW with partially encased composite columns. Seismic tests on seven specimens were performed, revealing that the SPRCCW with diagonal distribution reinforcement exhibited a 6.5% increase in cracking load and a 13.6% increase in ductility compared to those with orthogonal distribution reinforcement. Considering that the SPRCCW might be subjected to combined tension-bending actions, tests on seven specimens under tension-bending loads were conducted by Wang et al. [36]. Besides, the stud performance was investigated by Qi et al. [37]. Based on the numerical analysis,

the stud shear force demand was proposed.

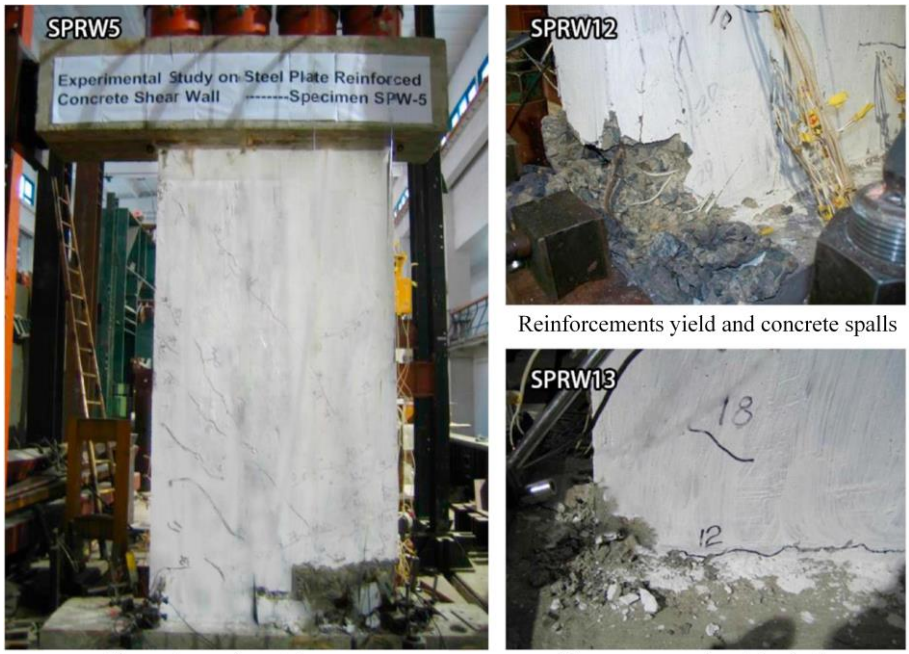

Fig. 6. Typical failure modes of SPRCCW under cyclic lateral loads [18].

With the development of material, high-performance material has been introduced in the SPRCCW. Seismic behavior of three specimens with varying steel plate yield strengths was investigated by Lou et al. [38]. It was indicated that the higher steel yield strength could increase the yield and ultimate loads and corresponding displacements of the wall, but it had negative effects on the ductility. Xiao et al. [39] carried out cyclic tests on 18 SPRCCWs with high-strength concrete, revealing that the performance of SPRCCW with high-strength concrete was improved obviously. Jiang et al. [40] also conducted tests on SPRCCW with high-strength concrete, and similar test results were obtained. During the test, the composite wall showed smaller and more dispersed cracks compared to the traditional RC shear walls. Both Xiao et al. [39] and Jiang et al. [40] suggested that the axial compression ratio should be kept below 0.5. The gangue concrete was introduced into SPRCCW by Zhang et al. [41]. It was concluded from the test that the SPRCCW with gangue concrete had excellent load-bearing capacity and ductility, accompanied by limited strength and stiffness degradations.

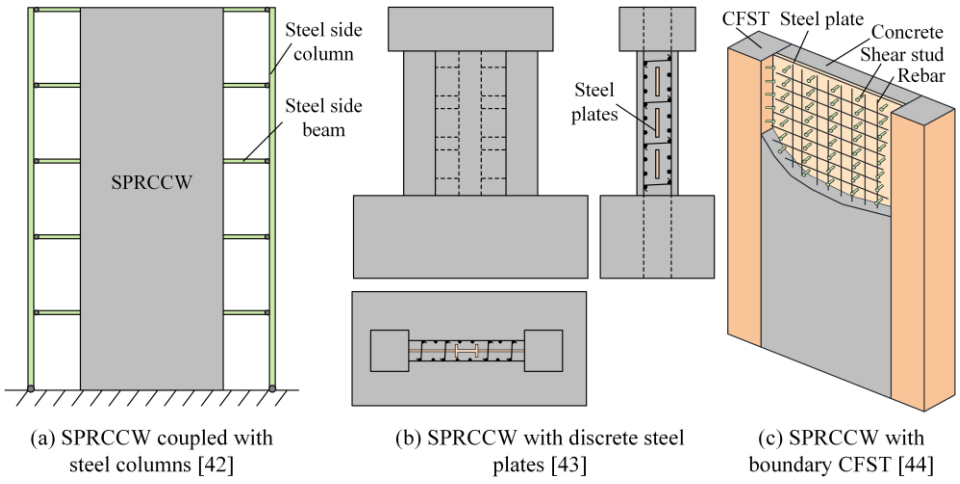

Fig. 7. New forms and constructions of SPRCCW.

New forms and constructions were proposed to further improve the performance of SPRCCW. By combining the SPRCCW with steel side columns, a 1/4 scaled five-story specimen was tested under

cyclic lateral loads by Ma et al. [42], as presented in Fig. 7(a). The coupled system exhibited excellent ductility, deformation capacity, and energy dissipation capacity. To simplify fabrication, Dong et al. [43] suggested a novel construction of SPRCCW using multiple smaller steel plates, as shown in Fig. 7(b). Seismic tests revealed that the wall demonstrated a remarkable capacity for energy dissipation. It was known that the concrete was easy to crush under large deformation. To offer this challenge, boundary CFST columns were used by Hu et al. [44] (Fig. 7(c)). The test phenomena revealed that the concrete crushing was significantly improved.

Another effective method was to use corrugated steel plates. Wang et al. [45, 46] investigated the behavior of SPRCCWs with embedded corrugated steel plates. The existence of corrugations enhanced the interaction between steel plates and concrete, resulting in improved initial stiffness, ductility, and energy dissipation capacity. SPRCCWs with vertical corrugated plates exhibited higher load-bearing capacity than SPRCCWs with horizontal corrugated plates. On this basis, Li et al. [47] analyzed the stress distribution of SPRCCW with vertical corrugated plates, and design formulas were proposed to predict the curvatures of the wall. To fully develop the capacity of steel plates and boundary columns, Luo et al. [48] suggested that the shear ratio of the column to the steel plate should to be larger than 1.45. Moreover, Song et al. [49] and Wang et al. [50] investigated the bond-slip performance between corrugated steel plates and concrete with and without studs, respectively. Bond-slip constitutive models were then established, showing good accuracy with test results. Numerical analysis on the shear resistance of the SPRCCW was carried out by Zhou et al. [51]. The impacts of the shear span ratio, steel ratio, concrete strength, axial compression ratio, and reinforcement ratio were evaluated.

3.3 Fire resistance

Xie et al. [52] studied the cyclic performance of SPRCCWs before and after fire exposure. As illustrated in **Fig. 8**, the spalling of concrete occurred in all specimens in the fire test, and the concrete spalling in SPRCCW was more serious than that in the traditional RC shear wall. Compared with the SPRCCW using an entire steel plate, the discrete steel plates effectively mitigated the propagation of diagonal cracks and the influence of fire exposure was less significant, which exhibited flexural failure. Although the load-bearing capacity of the SPRCCW were reduced due to the high temperature, the energy dissipation capacities were similar for SPRCCWs before and after fire exposure when the the drift ratio was less than 1/120.

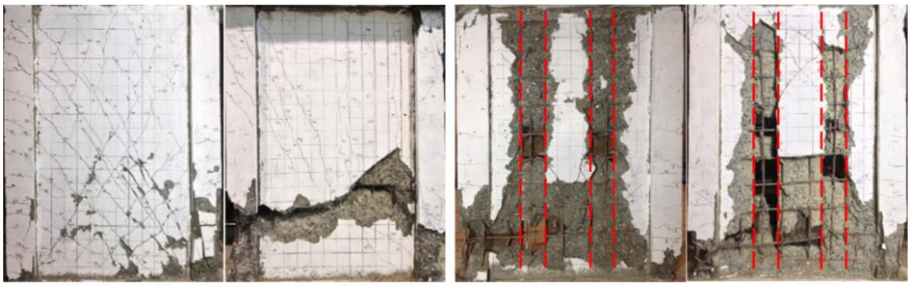

Fig. 8. Cracking pattern of walls under fire [52].

3.4 Dynamic Performance

A numerical analysis was investigated by Ren et al. [53] to study the dynamic performance of a 20-story building with SPRCCWs. The SPRCCW was simulated by a multilayer shell model, and the simulation results indicated that the internal force redistribution could significantly influence the behavior of the structures. Moreover, nonlinear numerical analysis on the seismic responses of four-story and six-story buildings using SPRCCWs was conducted by Dey and Bhowmick [54]. It was observed that the period of the building obtained from the existing design codes was shorter than that obtained from the numerical analysis. A modified formula to predict the fundamental period of SPRCCWs was then proposed.

4 Research on Double-skin Flat Plate Composite Wall

The DFPCW is the most widely used composite wall [55, 56]. The DFPCW was first applied as the floor in marine structural systems [57, 58], and then it was developed in residential and office buildings as lateral resistance components, attracting the attention of researchers. The DFPCW can fully develop the advantage of steel and concrete. Additionally, shear connectors are employed to ensure the interaction between steel and concrete. As shown in Fig. 9, different types of shear connectors are used in DFPCWs, including tie bar [59], shear stud [60], T-shaped stiffener [61], intermediate bolt [62], J-hook [63] and batten plate [23]. Studies on the performance of DFPCW under different loads have been conducted.

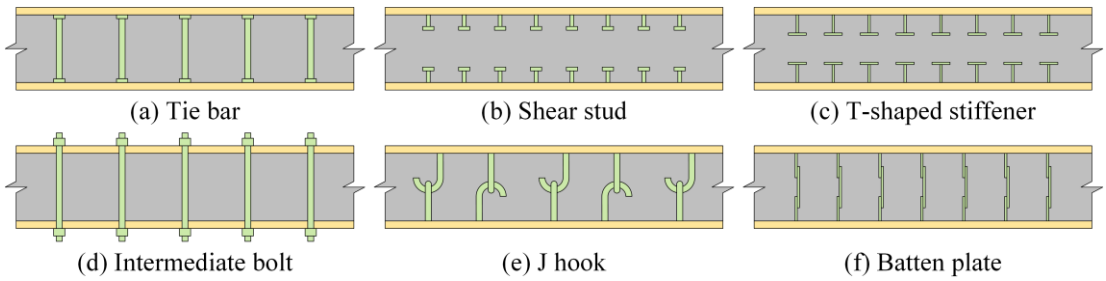

Fig. 9. DFPCWs with different shear connectors.

4.1 Compression Performance

The performance of DFPCWs under axial loads has been widely considered by researchers. In 1998, axial compression tests on DFPCWs with tie bars were conducted by Takeuchi et al. [64]. The structure exhibited high ultimate resistance and great ductility. Furthermore, they conducted an analysis on the failure mechanism of the composite wall.Yan et al. [25, 65, 66] conducted tests on DFPCWs with different shear connectors, including C-shaped channel steel, J-hook, and shear studs, and the typical failure mode is described in Fig. 10. The load-bearing capacity of DFPCWs can be increased by enhancing the height of headed studs and the thickness of steel plates. Notably, the impact of steel plate thickness is more obvious when the length of headed studs was short. The stability performance under axial compression was studied by Qin et al. [67], who utilized the steel truss composed of angle steel and kinked rebar as shear connectors, as depicted in Fig. 11(a). Increasing the thickness of steel plate effectively delayed its local buckling, thereby enhancing the buckling stress and axial stiffness. As presented in Fig. 11(b), Shi et al. [61] introduced a novel type of DFPCW using steel-bars truss as connectors. The axial compression tests demonstrated that the steel-bars truss effectively restrained local buckling of the external steel plates. Stability tests on DFPCWs with intermediate bolts were carried out by Chen et al. [68], and when the height-to-depth ratio was larger than 12, overall instability could be observed accompanied by the local buckling of steel plates.

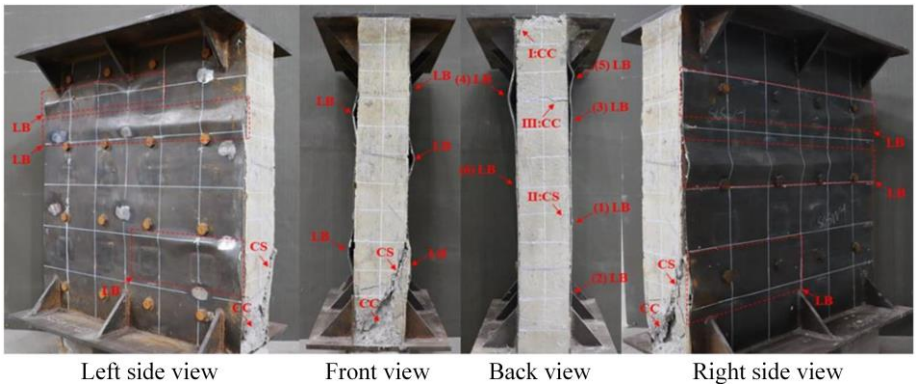

Fig. 10. Typical failure mode of DFPCW under axial compression [66].

Due to the poor stability of the external steel plates, the local buckling performance of steel plates was concerned by researchers. The axial compression test on ten specimens was carried out by Yang et al. [69] to investigate the impacts of key parameters on the axial performance of DFPCWs, including the width-to-thickness ratio of steel plate, spacing between shear studs and stud arrangement. Fig. 12

illustrates the local buckling deformation of steel plates observed in the tests. Combined with numerical analyses, it was suggested that the shear connector spacing to the steel plate thickness (s/t) should be less than $0.91\sqrt{E_s/f_y}$, where E_s is and f_y are the elastic modulus and yield strength of steel plate. Hu et al. [70] designed 12 specimens with intermediate bolts and conducted axial compression tests, and a calculation formula to present the ultimate and residual resistances of steel plates were proposed. The correlation between the shear stud stiffness and the local buckling performance of DFPCWs was studied by Harmon and Varma [71], revealing that the buckling mode of steel plates was significantly affected by the shear stud stiffness. Axial compression tests on DFPCWs with different shear connectors were carried out by Shi et al. [72, 73], demonstrating that the limit of s/t could be taken as $0.91\sqrt{E_s/f_y}$ for DFPCWs with shear studs, while the limit of s/t could be increased to $1.67\sqrt{E_s/f_y}$ for the DFPCW with both shear studs and additional stiffening ribs.

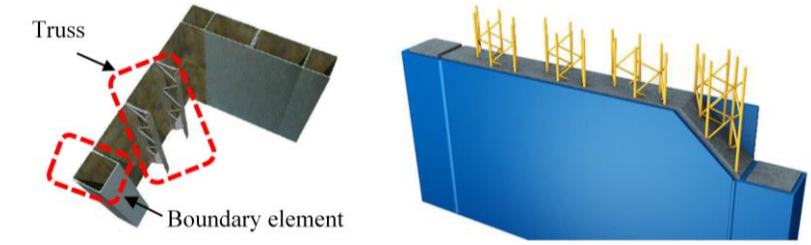

(a) DFPCW using steel truss [67] (b) DFPCW using steel-bar truss [61]

Fig. 11. DFPCW with new types of shear connectors.

(a) Front view (b) Back view

Fig. 12. Local buckling failure of DFPCW [69].

4.2 Cyclic Performance

As an excellent lateral resistance component, the seismic performance of DFPCWs is worth studying. Ozaki et al. [74] derived the calculation formula of the in-plane shear resistance of the DFPCW. The accuracy of this formula was successfully validated against the test results. The seismic performance of isolated and coupled DFPCWs with I- and T-shaped sections was experimentally explored by Eom et al. [62]. The study revealed that the failure of coupled DFPCWs was mainly attributed to the local buckling of steel plates and the weld fracture between the composite walls and coupling beams, as illustrated in Fig. 13. Nie et al. [23] conducted seismic tests on DFPCWs with vertical stiffeners and two boundary CFST columns, and high-strength concrete was considered. The results demonstrated that the reasonable arrangement of vertical stiffeners effectively mitigated the occurrence of local buckling in steel plates. Yan et al. [75] developed a new DFPCW with shear studs and boundary elements, which proved to improve the ductility of tall buildings, and all specimens showed local buckling of steel plates, fracture of boundary column, and crush of concrete. Moreover, the cyclic performance of DFPCWs with steel-bar space trusses and boundary CFSTR columns was experimentally investigated by Shi et al. [76], and a theoretical formula to predict the lateral resistance was presented.

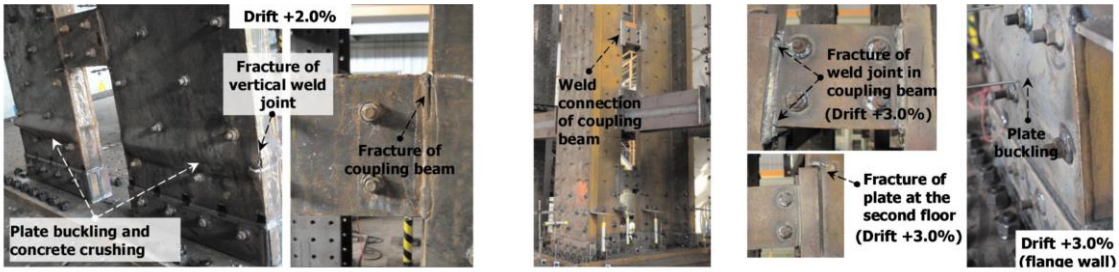

(a) Coupled DFPCWs with I-shaped section (b) Coupled DFPCWs with T-shaped section

Fig. 13. Failure mode of DFPCW [62].

4.3 Fire Resistance

The safely of structures exposed to fire has attracted much attention [77]. Fire tests on 12 DFPCW specimens were conducted by Wei et al. [78]. As depicted in Fig. 14, three typical phenomena were observed in the tests for the composite wall uniformly exposed to fire, including local buckling of steel plates, weld fracture, and global instability. For the composite wall exposed to single-sided fire, no obvious damage could be observed at 2.5 hours of fire exposure. Taghipour et al. [79] carried out numerical analyses to investigate the impact of key parameters on the fire resistance of the DFPCW. To enhance the failure time of the composite wall, it was suggested that the ratio of shear connector spacing to the steel plate thickness (s/*t*) should be less than $1.2\sqrt{E_s/f_y}$. Hu et al. [80] found that the out-of-plane stiffness of the composite wall was significantly affected by the fire exposure. A fitting formula to calculate the initial out-of-plane stiffness was presented. Besides, Du et al. [81] performed fire tests on DFPCWs with truss connectors. The test results indicated that the fire resistance of the wall was significantly influenced by the axial compression ratio and truss spacing.

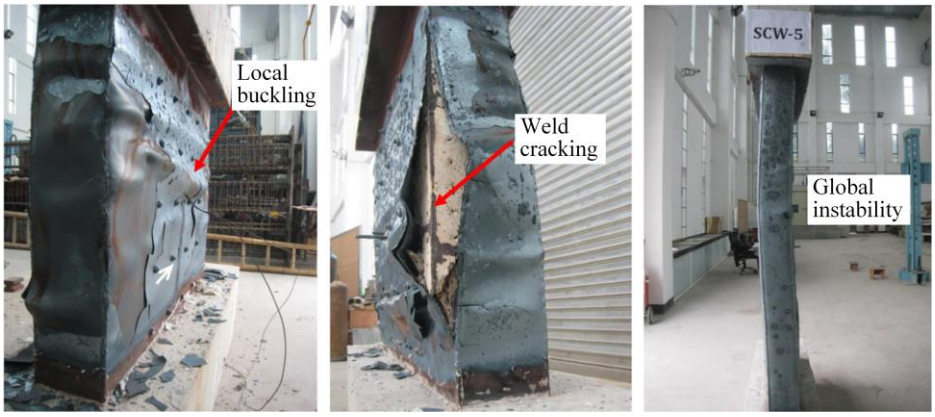

Fig. 14. Typical phenomena of DFPCW under fire exposure [78].

4.4 Flexural Resistance

McKinley and Boswell [82] conducted three-point bending tests on 16 specimens of DFPCW. For DFPCWs with tie bars, the failure of composite wall primarily attributed to the occurrence of local buckling in steel plates, while the DFPCWs with shear studs exhibited failure as a result of the shear studs pulling out of the concrete. The test results proved that the DFPCW with tie bars showed higher resistance and larger deformation compared to the DFPCW with shear studs. Besides, Sener et al. [83, 84] investigated the flexural performance of DFPCWs experimentally. The investigation revealed that the out-of-plane flexural strength of the structure was not influenced by the shear span-to-depth ratio and slenderness of steel plates, while the yield strength of steel plates had a significant impact. Varma et al. [85] study the flexural behavior of DFPCW in nuclear structures. It was suggested that the tensile strength and spacing of shear connectors should be carefully designed to prevent non-ductile failure of the wall. A four-point bending test was conducted by Yang et al. [86] to evaluate the buckling behavior of steel plates in DFPCWs under bending loads. It was indicated from test results that the stiffening ribs and tie plates could significantly improve the buckling stress of the steel plates, as described in **Fig. 15**.

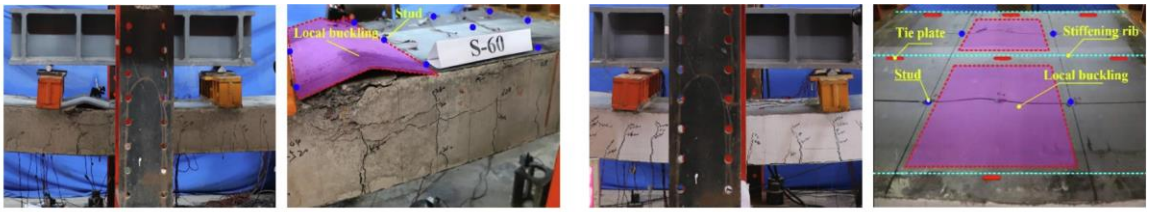

(a) DFPCWs without stiffening ribs and tie plates (b) DFPCWs with stiffening ribs and tie plates

Fig. 15. Failure mode of DFPCWs under flexural loads [86].

5 Research on Double-skin Corrugated Plate Composite Wall

The DCPCW was first proposed by Wright et al. [87], serving as the flooring system. As shown in **Fig. 16**, various types of corrugated plates have been applied in the DCPCW, including trapezoidal corrugation, sinusoidal corrugation, and re-entrant corrugation.

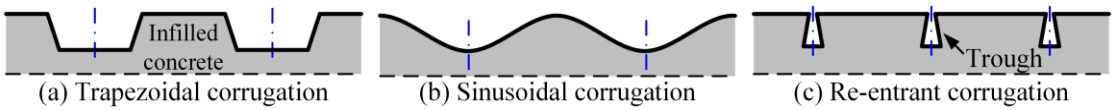

(a) Trapezoidal corrugation (b) Sinusoidal corrugation (c) Re-entrant corrugation

Fig. 16. Types of corrugations.

5.1 Compression Performance

Due to the special section shape of DCPCWs, the sectional strength and stability performance under axial compression were studied by researchers. In 1998, axial compression tests were carried out by Wright [88] to analyze the failure mode of DCPCWs. The ultimate resistance of DCPCW was affected by the local buckling of corrugated steel plates and section shape of concrete. A design formula to evaluate the sectional strength of DCPCW was then proposed, where a reduction factor was introduced to consider the influence of the above two factors. In engineering practice, openings for doors and windows are required, which may lead to the perforation of DCPCW. To investigate the axial compression performance of pierced DCPCWs, tests on 19 specimens were conducted by Hossain et al. [89]. The influence of corrugation dimensions, types of shear connectors, opening dimensions, and strength enhancement devices are evaluated. It was concluded that strengthening the boundary of the opening was the most effective approach to improve the behavior of pierced DCPCWs. Uy et al. [90] conducted tests on the DCPCW with re-entrant corrugation subjected to eccentric compression, where the local buckling of the corrugated plate was observed. On this basis, Tong et al. [91, 92] conducted numerical and theoretical analyses to to further examine the performance of DCPCWs. The analyses concluded that the material strength, wall depth, and steel plate thickness had positive effects on the axial and bending resistance of the wall. The interaction curves between axial and flexural capacities were then proposed.

As described in Fig. 17, a new type of DCPCW with boundary CFST columns and intermediate bolts was proposed by Guo et al. [26] in recent years. It was found from the test and simulation by Zhu et al. [28] that the corrugated steel plate between bolts was prone to buckle, which was described in Fig. 18(a). Therefore, the axial resistance of the wall was proposed, where the stability coefficient of the corrugated steel plate was considered. Zhou et al. [93] studied the performance of this new type of composite wall subjected to combined axial compression and in-plane bending. A theoretical model was presented to evaluate the cooperative effect between corrugated steel plates, concrete, and boundary elements, and the *N-M* correlation curve was presented. Moreover, the stability performance under axial compression was carried out by Guo et al. [26], as presented in Fig. 18(b). Combined with stability tests and numerical simulations, the stability curve was proposed. For T-shaped DCPCW, axial compression tests and numerical analysis were conducted by Wang et al. [94] to further investigate the performance of the composite wall under axial loads, bending loads, and combined axial and bending loads. The numerical results revealed that the load shared by steel plates ranged from 50% to 80% subjected to eccentric compression. Furthermore, Wang et al. [95, 96] also evaluated the flexural and flexural-torsional buckling behavior of T-shaped DCPCW under axial loads. The stability design method was then developed. Besides, the stability performance under combined axial compression and biaxial

bending loads was investigated using the same method [97]. Condiering the restraint provided by the infilled concrete against the inward buckling of corrugated steel plates in DCPCWs, the corrugated steel plate between intermediate bolts was simplified as a four-edge fixed steel plate by Wang et al. [27]. The stability curve of the four-edge fixed steel plate was proposed.

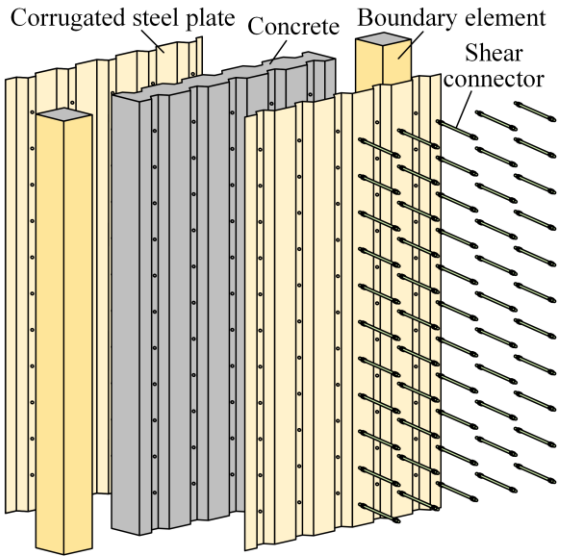

Fig. 17. Diagram of DCPCW with boundary CFST columns.

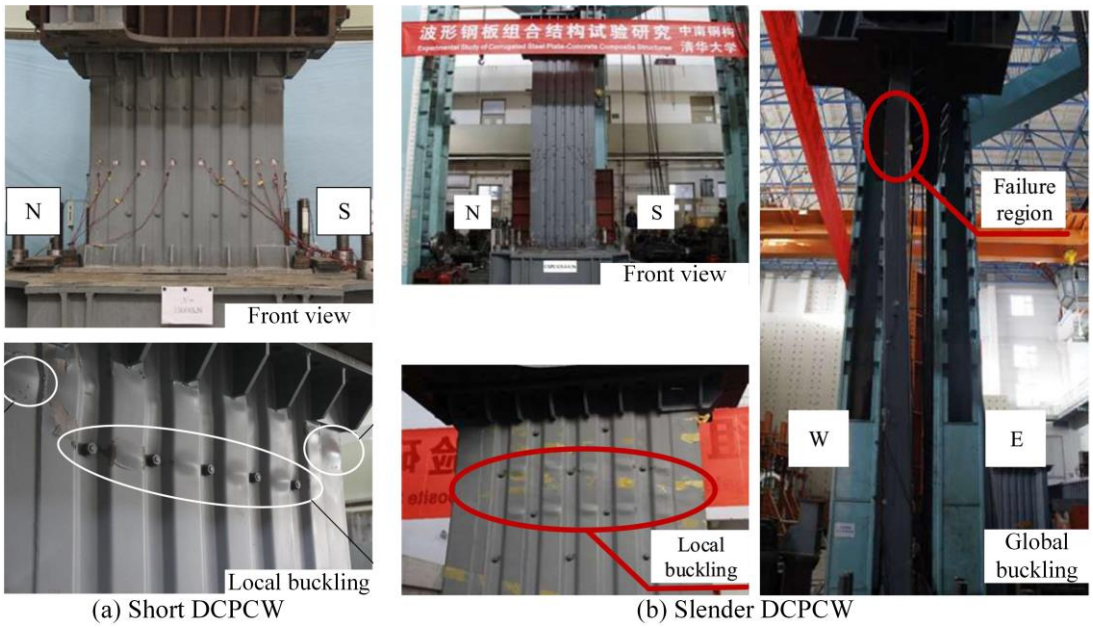

Fig. 18. Failure modes of DCPCW under axial compression [26, 28].

5.2 Cyclic Performance

As a lateral resistance component, the performance of DCPCW under shear loads was analyzed. Hossain and Wright [98-100] conducted shear tests on corrugated concrete plates and analyzed their failure modes. On this basis, shear tests on DCPCWs were performed and the theoretical models to calculate the shear capacity and initial stiffness of DCPCWs were proposed. Rafiei et al. [101] studied the shear behavior of DCPCWs using intermediate bolts. It was found that increasing the intermediate bolt number could increase the shear capacity of the DCPCW until the critical bolt spacing is reached, where the yielding of the corrugated plate occurred before buckling. The high-performance concrete was introduced into DCPCW instead of normal concrete by Rafiei et al. [102]. The test results proved that high-performance concrete could improve the ductility of DCPCWs.

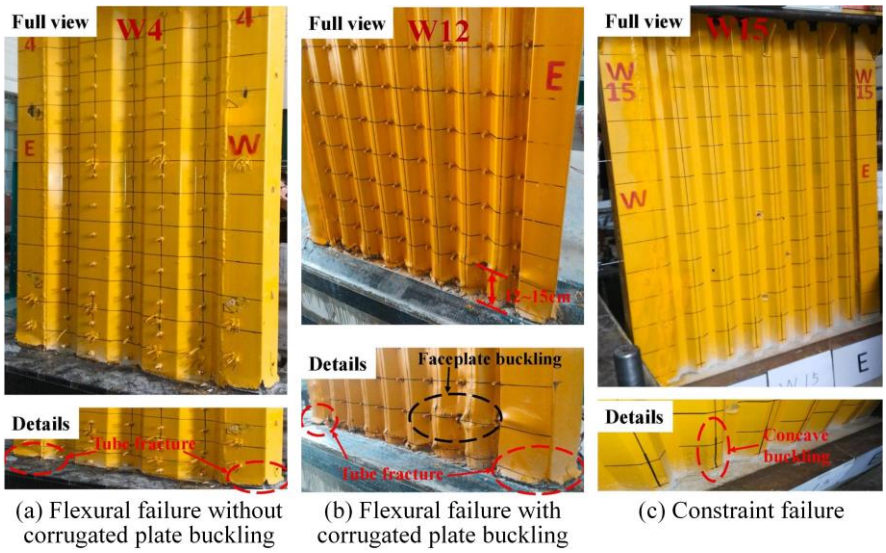

(a) Flexural failure without corrugated plate buckling (b) Flexural failure with corrugated plate buckling (c) Constraint failure

Fig. 19. Failure modes of DCPCW [103].

Based on the studies of the shear performance of DCPCWs, the seismic performance was further investigated. Hossain et al. [104] conducted tests on six specimens subjected to cyclic lateral loads, revealing that the utilization of mild-strength steel enhanced the ductility of the wall. Zhao et al. [105] compared the seismic performance of DCPCWs and DFPCWs. DCPCWs showed better initial stiffness and energy dissipation capacity than DFPCWs when the bolt spacing was 50% larger than the limit in design codes. The seismic behavior of DCPCW with boundary CFST columns shown in Fig. 17 was evaluated by Zhu et al. [106]. The test results on eight specimens revealed that the specimens were all subjected to compression-bending failure. Increasing the shear span ratio could enhance the ductility of the wall, while it was negatively correlated with the shear resistance. On this basis, the theoretical formula was developed to predict the ultimate resistanc of DCPCWs. Moreover, Zhou et al. [103] conducted hysteretic tests on 15 specimens, and three types of failure modes were concluded as described in Fig. 19. The results confirmed that the DCPCW with vertical corrugations exhibited much better hysteretic performance than the DCPCW with horizontal corrugations.

5.3 Fire Resistance

Le et al. [107] investigated the axial compression performance of the DCPCW at ambient and elevated temperatures. The tests indicated that the DCPCW exhibited ductile failure at ambient temperature, but the ductility of the wall decreased with the increase of temperature. Besides, the temperature also showed a negative effect on the axial resistance of the wall. Since the composite wall was subjected to single-sided fire, the effective centroid would be affected by the temperature gradient, which influenced the failure plane of concrete. To further understand the performance of DCPCWs exposed to single-sided fire, Le et al. [108] proposed an analytical model considering the non-uniform stiffness and non-linear temperature gradient. The proposed model exhibited good accuracy with the experimental results, which could be used to predict the stress and curvature of the structures.

5.4 Impact Performance

Rafiei et al. [109] studied the impact shear resistance of DCPCWs. It was found that the shear strength after impact loads was not reduced and the stiffness was only reduced by 8%. Thus, the DCPCW had great impact shear resistance.

6 Research on Multi-celled Concrete-filled Steel Tubular Wall

According to previous studies, the diaphragm connectors ensure the development of composite action in MCFSTWs. As illustrated in Fig. 20, various types of MCFSTW have been developed. Many scholars have carried out detailed research on its performances, including axial compression

performance, seismic performance, fire resistance, and joint performance.

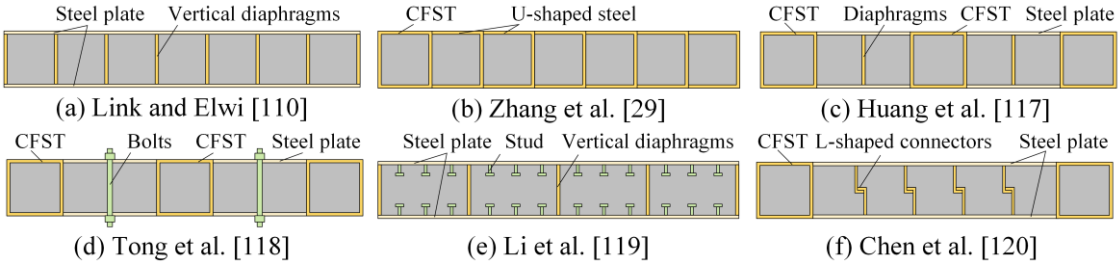

Fig. 20. Different types of MCFSTW.

6.1 Compression Performance

In 1995, Link and Elwi [110] conducted tests on MCFSTW which was used in offshore structures. Considering the action of waves and moving ice, the MCFSTW was tested under axial and out-of-plane loads, proving the good ductility of the composite wall. Guo et al. [111] and Li et al. [112] respectively performed tests on MCFSTWs with normal concrete and self-compacting concrete, and the deformations are presented in Fig. 21. It was found that the strength failure occurred for stub MCFSTWs accompanied by obvious local buckling of steel plates. Furthermore, Li et al. [112] employed ultrasonic testing to monitor the progression of concrete damage. The residual strength and ductility index were investigated by Zhang et al. [113], and it was concluded that these two parameters demonstrated positive correlations with the confinement factor. Based on the tests and numerical simulations, fitting formulas were presented to predict these two parameters.

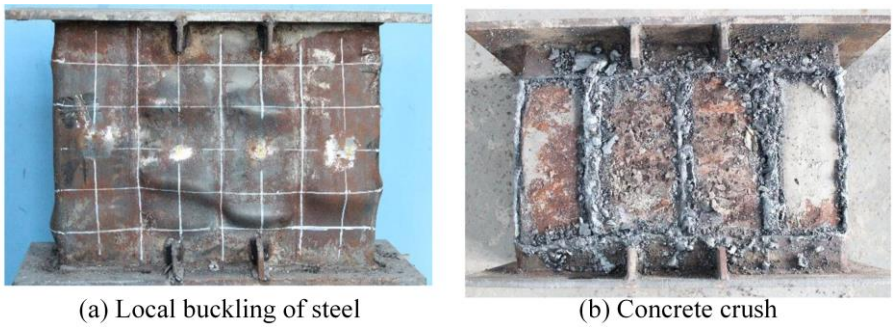

Fig. 21. Finial deformation of MCFSTW under axial compression [111]

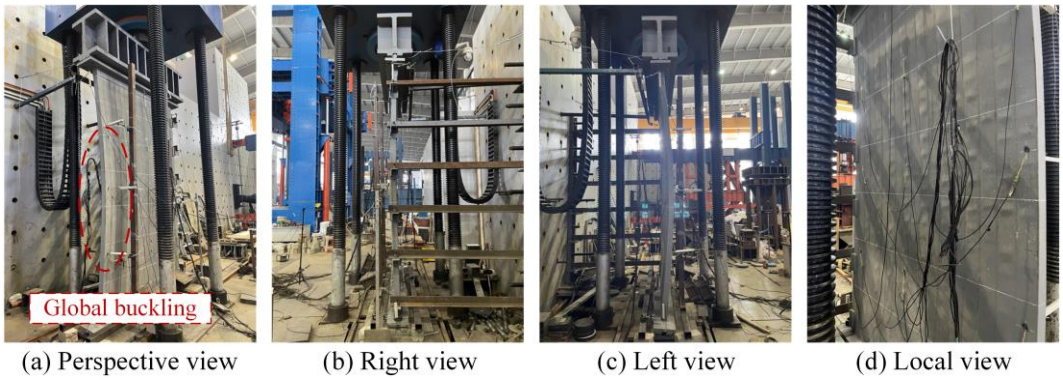

Fig. 22. Stability performance of MCFSTW with three simply-supported edges [17].

For slender MCFSTWs, stability tests under axial compression were conducted by Wang et al. [114] and Zhou et al. [31]. Parametric analysis showed that increasing steel plate thickness and decreasing material strength could improve the stability performance of the MCFSTW, while it was hardly affected by the wall width. Besides, Zhou et al. [17] conducted stability tests on MCFSTWs with three simply-supported edges under axial compression. As shown in Fig. 22, The three specimens all exhibited global instability where the out-of-plane deflection of the free edge was observed. By using

orthotropic plate theory, the elastic buckling load was proposed, and then the stability curve was presented. By using the same theoretical method, the stability performance of MCFSTWs with four simply-supported edges was evaluated [115].

6.2 Cyclic Performance

Zhang et al. conducted experimental tests to assess the mechanical properties of the MCFSTW when subjected to combined axial compression and lateral cyclic loads.

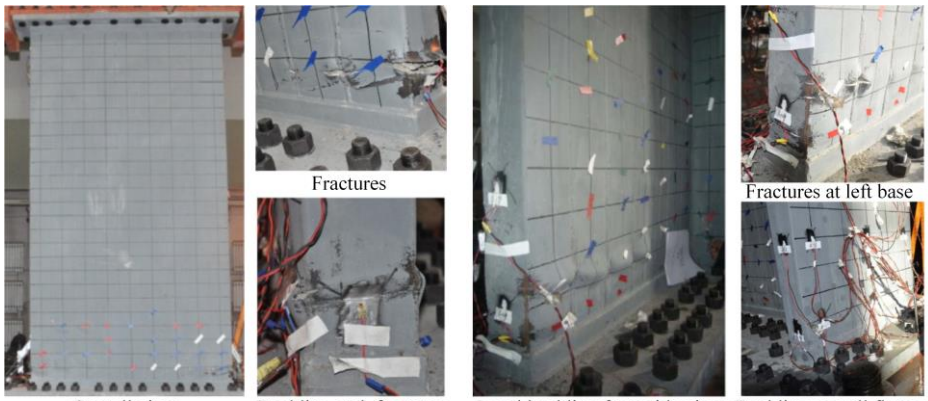

Fig. 23. Failure modes of MCFSTW under cyclic loads [29, 30].

Zhang et al. [29, 30] carried out tests to evaluate the mechanical properties of the MCFSTW when subjected to combined axial compression and lateral cyclic loads, including seven specimens with an I-shaped section and five specimens with a T-shaped section. Combined with the failure modes shown in Fig. 23, the energy dissipation capacity, ductility, stiffness, and ultimate strength of the wall were analyzed in detail. The results revealed that an increase in the axial compression ratio resulted in accelerated degradation of strength and stiffness, while it has little effect on the yield and peak strengths. It was widely recognized that the skeleton curves obtained from tests generally contained the second-order effect of axial loads which was calculated separately in the structural design software. To apply the test results to structural design, Zhou et al. [116] proposed a method to modify the skeleton curve that excluded the second-order effect, and a more accurate ductility for practical design was obtained. A new type of MCFSTW consisting of CFST columns and steel plates infilled with concrete was developed by Huang et al. [117]. The seismic tests on five specimens showed that the structure had good hysteretic performance. Subsequently, a fitting formula was presented to calculate the lateral bearing capacity of the wall, taking into account the confinement effect of the infilled concrete. Furthermore, tie-bolts were introduced into the MCFSTW by Tong et al. [118], and the tie-bolts were proved to suppress the local buckling half-wavelength of the steel plate. Based on test results, two simplified models of the hysteretic curves were presented. Li et al. [119] studied the performance of L-shaped MCFSTWs. The weld cracking was observed at the bottom end of webs when the wall flange was width, while only local buckling of webs occured for the MCFSTW with a narrow flange. Chen et al. [120-122] presented an innovative composite wall where the diaphragm was replaced by two L-shaped connectors. Theoretical formulas were developed to estimate the wall bending strength and the local buckling stress of the steel plate. To reflect the requirement of MCFSTWs under earthquake more accurately and reasonably, Wang et al. [123, 124] proposed a new loading protocol for quasi-static tests.

6.3 Fire resistance

Compared with the mechanical performance under other loads, the research works on the fire resistance of the MCFSTW are limited. Liu et al. [125, 126] conducted tests on eight specimens under axial loads when exposed to fire. The test indicated that the inner force distribution and the stress and strain distribution of the MCFSTW exhibited similarities to those of traditional CFST columns. Since the diaphragm connectors were inside the composite wall, they were not significantly affected by the fire. Thus, the presence of the inner diaphragm with lower temperatures was found to be crucial in

enhancing the load-bearing capacity of the wall and reducing the occurrence of local buckling in the steel plates. Combined with the test results and refined FE simulation results, a simplified calculation formula to predict the fire resistance of the MCFSTW and a method for determining the fire protection thickness were proposed.

6.4 Joint performance

Joint performance is a critical aspect of structural design. Recognizing that butt joints are susceptible to tensile fractures, Tong et al. [127] introduced a novel butt joint configuration, where the T-shaped connector was applied. Tensile tests on 12 specimens were carried out, among which six specimens had web plates and the other six did not have web plates. The test results demonstrated a significant enhancement in the tensile strength and ductility of the butt joint when the additional welding seam was introduced between the web plate and connector. For wall-beam joints of MCFSTW, Tong et al. [128] explored its bending strength and stiffness. According to the yield line analysis, the design formulas to calculate the initial stiffness and bending resistance were proposed. The theoretical formulas proved to have good accuracy with simulation results. Guo et al. [129] conducted tests on four MCFSTW-beam joints with double side plates. The results proved that both types of joints with discrete and consecutive double side plates could provide satisfactory collapse resistance. To improve the prefabrication degree of the joint, An et al. [130] proposed an anchored prefabricated wall-beam joint. Based on the hysteretic test on four specimens, the joint was confirmed to have good seismic performance. Besides, an innovative joint was investigated experimentally by Xu et al. [131] which could be used between replaceable coupling beams and walls. A design formula was presented to calculate the strength of this joint.

7 Research on multi-celled corrugated-plate CFST wall

7.1 Compression performance

As a new composite wall with excellent performance, the behavior of MC-CFSTW under axial compression was investigated by Tong et al. [33]. As shown in **Fig. 24**, it was evident that local buckling occurred in both the steel tubes and corrugated steel plates during the test. A numerical study was then conducted by Yu et al. [132]. Increasing the thickness and yield strength of the steel tube resulted in the increment of both the ultimate and residual strengths of the wall, while increasing corrugated cell width and wall depth could increase the ultimate strength of the wall but reduce its ductility. A formula to calculate the sectional strength of the MC-CFSTW was fitted, which was a function of the equivalent confinement factor of the wall. Furthermore, Tong et al. [133] explored the stability performance of the composite wall, and a stability test on six slender MC-CFSTWs was conducted. By comparing with the existing design curves, it was found that the formulas specified in design codes were not suitable for MC-CFSTWs. Therefore, a new stability curve was proposed with good accuracy. Li et al. [134] presented a novel type of MC-CFSTW, where the composite wall consisted of CFST components and corrugated plates connected alternately, and the CFST component was composited by two flat plates and two corrugated plates infilled with concrete. Experimental and numerical analyses were conducted to study the axial compression behavior of the CFST components. The results revealed good composite action of the wall with strength indexes of all specimens exceeding 1.17.

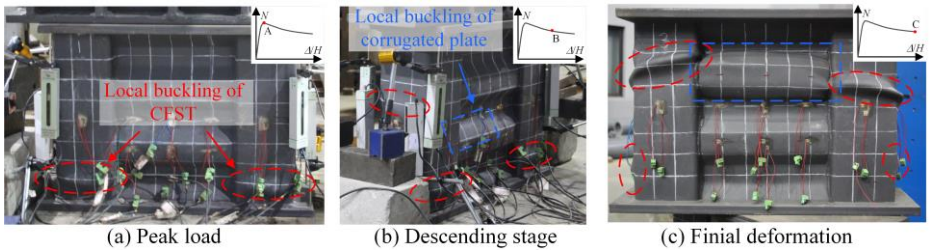

Fig. 24. Typical failure modes of MC-CFSTW under axial compression [33].

7.2 Cyclic performance

Except for the axial compression performance, the cyclic performance of MC-CFSTWs was also studied [135]. Based on the seven full-scaled specimens, the hysteretic performance of the wall was found to be significantly effected by the axial compression ratio. Specifically, global buckling failure occurred in the post-ultimate stage with the axial compression ratio larger than 0.55, as described in **Fig. 25**. Moreover, the ductility of the MC-CFSTW was compared with that of the MCFSTW developed by Tong et al. [118] and Zhang et al. [29]. Though the steel consumption was reduced by about 20%, the ductility of the MC-CFSTW was similar to that of the MCFSTW. In the study conducted by Tong et al. [136], eight specimens of MC-CFSTWs using interval flat plates subjected to cyclic loads with different axial compression ratios were tested. The MC-CFSTWs with boundary flat plates demonstrated flexural failure modes in the test, whereas those with boundary H-shaped or CFST columns exhibited shear failure modes.

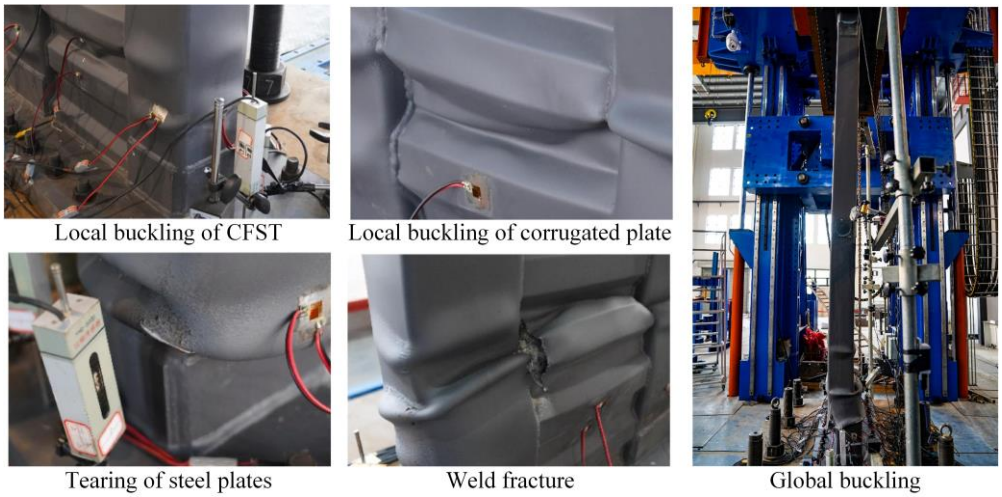

Fig. 25. Typical failure modes of MC-CFSTW under cyclic loads [135].

7.3 Flexural performance

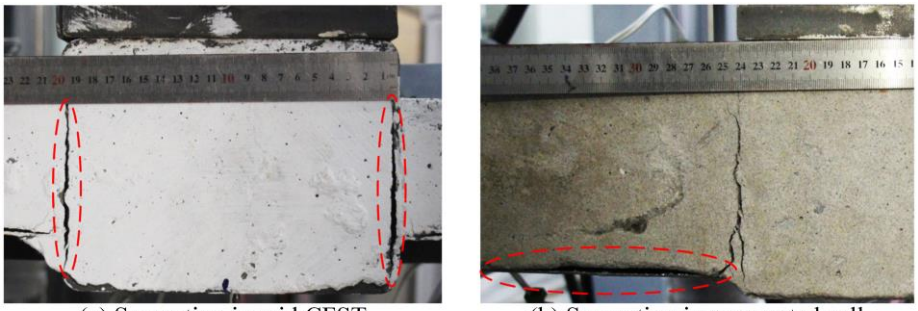

Fig. 26. Typical failure modes of MC-CFSTW under flexural loads [32].

The MC-CFSTW could also be applied in underground pipe gallery projects to subject withstand out-of-plane loads. The experimental study was performed to study the out-of-plane flexural performance of the wall [32]. As described in **Fig. 26**, the mid CFST showed significant local deformation due to the tensile force exerted by the corrugated steel plate. Therefore, the deflection of the specimen was regarded as the combined action of overall bending deformation and local deformation. Based on the theoretical analysis, the prediction formulas to calculate the initial stiffness and ultimate bending capacity were proposed.

7.4 Joint performance

Duan et al. [137] proposed a wall-beam joint for MC-CFSTWs. Numerical analysis revealed that the width-to-thickness ratio of steel tubes and the hole diameter of the horizontal diaphragm had negative effects on the rotational stiffness of the joint. Conversely, increasing the axial compression ratio and concrete strength enhanced its rotational stiffness. Moreover, the yield strength of steel plates

had no influence on the joint stiffness, which could significantly affect the joint bending strength. Utilizing the yield line analysis method, a design formula was presented to calculate the bending resistance of the joint.

8 Design formulas

8.1 Shear resistance

Different types of composite walls have different methods to calculate their shear resistance. For SPRCCW, the superposition principle is applied, and the design formula can be expressed as

$$V = V_c + V_N + V_b + V_p + V_r \tag{1}$$

in which V is the shear capacity of the SPRCCW; V_c, V_b, V_p, and V_r are the shear capacities of concrete, boundary elements, embedded steel plate, and steel rebars, respectively; and V_N is the contribution of axial compression loads. The calibration factors of different components were proposed according to the numerical and experimental results, and Eq. (1) can be further expressed as

$$V = \alpha_1 f_t d_w b_w + \alpha_2 N_0 + \alpha_3 f_{yb} A_b + \alpha_4 f_{yp} A_p + \alpha_5 f_{yr} A_r h_r / s \tag{2}$$

in which f_t is the tensile strength of concrete; d_w and b_w are the wall depth and effective width, respectively; N_0 is the axial load, which is less than $0.2 f_c b_w d_w$; f_{yb} is the yield strength of boundary elements; A_b is the cross-sectional area of single-side steel boundary column, taken as the smaller area of two boundary columns; f_{yp} and A_p are the yield strength and area of embedded steel plate, respectively; f_{yr} and A_r are the yield strength and area of horizontal steel rebars, respectively; h_r is the configuration width of steel bar; s is the spacing between two horizontal steel rebars; and α_1 to α_5 are the calibration factors.

The calibration factors specified in design codes and literature are summarized in **Table 2**. It is found that the design formula specified in the code cannot predict the shear capacity accurately with the development of new types of structures. However, these calibration factors are obtained by fitting tests and FE results, which are only applicable to specific structures and lack universality. It is still worthy of further study.

Table 2. Design formulas for the shear capacity of SPRCCW

Type	Design formula					Other specifications					
	α_1	α_2	α_3	α_4	α_5	ρ	ρ_r	f_{yp}	f_{cu}	n_d	λ
JGJ 138 [138]	$\frac{0.5}{\lambda-0.5}$	$\frac{0.13}{\lambda-0.5}$	$\frac{0.3}{\lambda}$	$\frac{0.6}{\lambda-0.5}$	1	< 6.7%	0.3%	355~420	30~60	—	—
Xiao et al. [39]	$\frac{0.67}{\lambda-0.5}$	$\frac{0.20}{\lambda-0.5}$	$\frac{0.6}{\lambda-0.5}$	$\frac{0.45-2.5\rho}{\lambda-0.5}$	1	< 5.6%	0.59%	369~407	74~91	0.25~0.34	1.0
Zhang et al. [41]	$\frac{0.5}{\lambda-0.5}$	$\frac{0.13}{\lambda-0.5}$	$\frac{0.3}{\lambda}$	$\frac{0.293}{\lambda}$	1	3.3%	0.25%	235~355	48.3	0.3~0.5	1.0~2.0
Zhou et al. [51]	$\frac{1.52}{\lambda-0.5}$	$\frac{0.26}{\lambda-0.5}$	$\frac{0.3}{\lambda}$	$\frac{0.37-1.35\rho}{\lambda-0.5}$	$\frac{0.55}{\lambda}$	1%~7%	0.3%~1.0%	—	50~80	0.1~0.3	1.0~1.5
Wang et al. [45]	$\frac{0.5}{\lambda-0.5}$	$\frac{0.13}{\lambda-0.5}$	$\frac{0.3}{\lambda}$	$\frac{0.66\varphi_s}{\lambda-0.5}$	1	1.3%~2.7%	0.19%	292	47.6	0.15	1.0~2.0
Luo et al. [139]	$\frac{0.475}{\lambda-0.5}$	$\frac{0.1235}{\lambda-0.5}$	$\frac{0.15}{\lambda}$	$\frac{0.27\varphi_s}{\lambda-0.5}$	0.8	2.0%	0.19%	235~460	46.8	0.15	1.5

where λ is the shear span ratio of the composite wall; ρ is the steel plate ratio; φ_s is the stability coefficient of corrugated steel plates; f_{cu} is the cubic strength of concrete; and n_d is the axial compression ratio.

For the other four types of steel-concrete composite walls, it is recommended to disregard the contribution of concrete. As a result, the shear capacity can be expressed as

$$V = f_{vs} A_s \tag{3}$$

in which f_{vs} and A_s are the shear yield strength and area of the steel plate in the composite wall, respectively.

Besides, when the height-to-width ratio is large, the composite wall exhibits bending failure modes [18, 106, 136]. For the bending resistance of the steel-concrete composite wall, the sectional analysis method [19] was used. The position of the neutral axis could be calculated through the balance of forces. Based on the assumption of plane sections, the stress distribution was obtained, and hence, the bending moment of the sections was further calculated.

8.2 Axial compression resistance

The design formulas for determining the axial resistance of steel-concrete composite walls in existing codes are tabulated in **Table 3**, including AIJ [140], AISC360 [141], BS5400 [142], and EC4 [143].

Table 3. Design codes for steel-concrete composite structures

Design codes	Design formulas
AIJ	$N_u = A_s f_m + 0.85 A_c f_c'$, $f_m = \min\left\{ f_{ys}, 0.7 f_{us} \right\}$
AISC360	$N_u = A_s f_{ys} + 0.85 A_c f_c'$
BS5400	$N_u = 0.95 A_s f_{ys} + 0.45 A_c f_{cu}$
EC4	$N_u = A_s f_{ys} + A_c f_c'$

where f_c' and A_c are the compressive strength and cross-sectional area of concrete in the composite wall, respectively; f_{ys} and f_{us} are the yield strength and tensile strength of steel plate, respectively.

Based on the above design codes, the axial compression capacity can be expressed as

$$N = \beta_1 A_s f_{ys} + \beta_2 A_c f_c' \tag{4}$$

in which β_1 and β_2 are calculation factors.

Different calculation factors have been proposed for various forms of composite walls. For the SPRCCW, the concrete strength can be determined based on the cylinder compressive strength. However, for the other four types of composite walls, the concrete strength is often estimated using the confined concrete strength, considering the confinement effect of steel plate and steel reinforcement bars. Yan et al. [25, 65, 66] proposed a method for calculating concrete strength under the confinement of different shear connectors. The confined concrete theory proposed by Mander et al. [144] was suggested to determine the confined concrete strength [34]. For the steel material, it was suggested that the vertical stress should be reduced due to the confinement effect of steel on the concrete. However, it was difficult to determine the vertical stress of steel plates theoretically, and its value varied greatly from existing literature [33, 145]. In many studies, the strain gauge data observed in the test were used to determine the vertical strain of steel plates when the specimen reached peak load, thereby obtaining the vertical stress of the steel plates.

8.3 Stability resistance

The load-bearing capacity of the composite wall with large slenderness ratio is controlled by its stability. The stability curves of various types of composite walls are different. Chen et al. [68] suggested that the stability curve of DFPCWs with intermediate bolts could be calculated as:

$$\varphi = \begin{cases} 1 - 1.57\lambda_0^2 & \lambda_0 \le 0.215 \\ \dfrac{\Phi - \sqrt{\Phi^2 - 4\lambda_0^2}}{2\lambda_0^2} & \lambda_0 > 0.215 \end{cases} \tag{5}$$

$$\Phi = \lambda_0^2 + 0.1729\lambda_0 + 1.046$$

where λ_0 is the normalized slenderness ratio; and φ is the stability coefficient. However, due to the lack of experimental results, the stability curve with a normalized slenderness ratio greater than 0.6 should

be modified. Qin et al. [146] proposed the stability curve of DFPCWs with steel truss under axial compression through tests and numerical simulations, and the stability curve could be expressed as

$$\varphi=\begin{cases}1-0.41243\lambda_0^2 & \lambda_0\le 0.6\\ \dfrac{1}{1.0304+0.4\lambda_0^2} & \lambda_0>0.6\end{cases} \tag{6}$$

Similarly, Guo et al. [26] and Zhou et al. [31] proposed the stability curves of DCPCWs and MCFSTWs, respectively, as shown in Eqs. (7) and (8). Tong et al. [133] explored the stability performance of MC-CFSTWs, and the stability curve could be calculated by Eq. (9).

$$\varphi=\begin{cases}1-0.835\lambda_0^2+0.37\lambda_0^3 & \lambda_0\le 0.8\\ \dfrac{\Phi-\sqrt{\Phi^2-4\lambda_0^2}}{2\lambda_0^2} & \lambda_0>0.8\end{cases} \tag{7}$$

$$\Phi=\lambda_0^2+0.9\lambda_0+0.586$$

$$\varphi=\frac{1}{\Phi+\sqrt{\Phi^2-\lambda_0^2}} \tag{8}$$

$$\Phi=0.684\lambda_0^2-0.012\lambda_0+0.5$$

$$\varphi=\begin{cases}1 & \lambda_0\le 0.116\\ \dfrac{\Phi-\sqrt{\Phi^2-4\lambda_0^2}}{2\lambda_0^2} & \lambda_0>0.116\end{cases} \tag{9}$$

$$\Phi=1.36\lambda_0^2+0.13\lambda_0+0.98$$

The stability curves of different types of composite walls are compared in **Fig. 27**, revealing that the utilization of truss connectors significantly enhances the stability performance of DFPCWs. The stability curves of DCPCWs and MC-CFSTWs are close. However, when compared to MCFSTWs, both DCPCWs and MC-CFSTWs demonstrate worse stability performance.

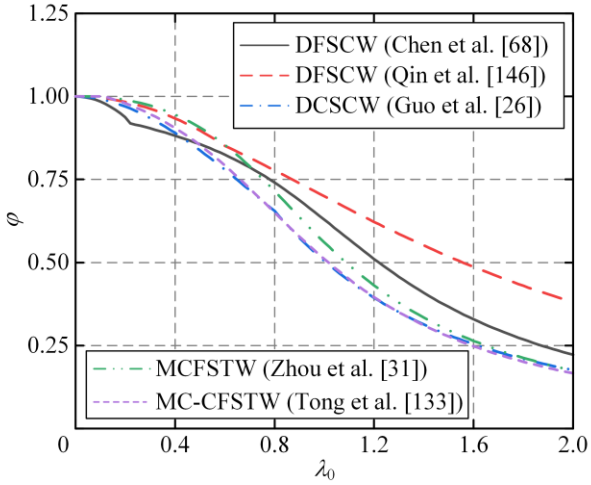

Fig. 27. Comparison of different stability curves

9 Future research perspectives

9.1 Pre-fabrication and modular construction

Pre-fabricated structures offer numerous advantages, including reduced material waste, environmentally friendly construction, flexible structural arrangements, high degree of industrialization, and rapid construction. Fabricated steel structures align with the concept of life-cycle design for green

buildings. The widespread application of pre-fabricated steel structures represents a significant way to achieve building industrialization. In recent years, research has increasingly focused on the prefabricated structure, but the absence of reliable design codes and standards limits its development. Additionally, modular construction has attracted increasing attention. Modular steel construction and modular concrete construction have been applied in many regions such as Hong Kong and Singapore, while modular composite construction is few and requires detailed scientific research for further advancements

9.2 High performance and sustainable materials

Researchers have conducted numerous analyses in recent years to investigate the mechanical properties of steel-concrete composite walls. However, the current studies focus on normal strength materials, with limited research on high performance and sustainable materials. High-strength materials have been extensively explored in CFSTs, enabling steel yield strengths of up to 780 MPa and concrete cylinder strengths of up to 190 MPa [147]. Consequently, high-strength materials can also be introduced in composite walls to further reduce cross-sectional dimensions and enhance the load-bearing capacities of the structural elements.

Furthermore, the utilization of lightweight concrete can effectively decrease the self-weight of structures, particularly in high-rise buildings. Previous investigations have revealed that concrete in SPRCCWs is prone to cracking under load. Therefore, the utilization of high-toughness concrete can help prevent cracks and enhance durability [148]. Moreover, recycled aggregate concrete agrees with sustainability goals and has attracted much attention [149-151], which can be used in composite structures. The existing literature shows limited investigations on composite walls using high performance and sustainable materials, which provides a direction for future research.

9.3 Load types and design provisions

Although existing studies have extensively analyzed the behavior of steel-concrete composite walls under different load conditions, there are clear gaps in the current literature. For instance, few studies were conducted on the effect of dynamic loads, which directly reflect the characteristics of structures during earthquakes. Additionally, the impact of thermal loads, impact loads, and explosion loads can be further explored as supplementary areas of research.

Moreover, the deficiency of standards significantly affects the application of steel-concrete composite walls. Despite the progress made in studying novel structural forms, an integrated system of design methods has not been formed. On one hand, the design formulas proposed in existing literature lack universality. On the other hand, the design formulas provided by current standards fail to fully reflect the advantages of the novel types of composite walls in load-bearing performance. Thus, comprehensive and universally applicable design methods that effectively reflect the benefits of innovative composite walls are required.

10 Conclusion

Compared to traditional reinforced concrete shear walls and steel plate shear walls, steel-concrete composite walls offer several advantages. These include high load-bearing capacity, good energy dissipation, and significant deformation capacity, making them ideal for high-rise buildings.

This review summarized the research on various steel-concrete composite wall types. We classified these walls into five categories based on their cross-section and the relative positions of steel and concrete. These categories include steel plate reinforced concrete composite wall (SPRCCW), double-skin flat plate composite wall (DFPCW), double-skin corrugated plate composite wall (DCPCW), multi-celled concrete-filled steel tubular wall (MCFSTW) and multi-celled corrugated-plate concrete-filled steel tubular wall (MC-CFSTW). The reviewed research highlighted several key findings:

(1) Limited research on non-static loads: Existing research primarily focuses on axial compression and cyclic performance, with less emphasis on the effects of dynamic, thermal, and impact loads.

(2) Concrete failure and confinement: For SPRCCW walls under axial compression, concrete

crushing and spalling can reduce structural ductility. However, walls where concrete is confined between steel plates (DFPCW, DCPCW, MCFSTW, and MC-CFSTW) exhibit limited concrete spalling due to the steel plates, leading to improved ductility.

(3) Seismic performance and influencing factors: The composite action between steel and concrete contributes to excellent seismic performance. While increasing the axial compression ratio reduces deformation capacity and ductility, a higher steel ratio enhances wall stiffness and strength.

(4) Connectors and their role: Connectors are instrumental in ensuring composite action between steel and concrete. Researchers are continuously developing new connector types to improve overall wall performance.

(5) Design considerations: Scholars have proposed design formulas for different composite wall types under various loads. While testing has verified the accuracy of these formulas to some extent, their universal applicability requires further investigation.

Future research directions to promote the wider use of composite walls include: pre-fabrication and modular construction techniques, exploration of alternative and sustainable materials, and the development of new design theories.

Acknowledgement

This study has been supported by Zhejiang Provincial Natural Science Foundation of China (Grant no. LR24E080002).

Conflicts of Interest

The authors declare that they have no conflicts of interest to report regarding the present study.

References

[1] Dong ZQ, Ji JH, Liu ZQ, Wu C, Wu G, Zhu H, Zhang P. I-shaped ECC/UHPC composite beams reinforced with steel bars and BFRP sheets. Sustain. Struct. 2023; 3(1): 000022. https://doi.org/ 10.54113/j.sust.2023. 000022.

[2] Wang WQ, Wang JF, Guo L. Mechanical behavior analysis of LEM-infilled cold-formed steel walls. Sustain. Struct. 2022; 2(1): 000013. https://doi.org/10.54113/j.sust.2022.000013.

[3] Papavasileiou GS, Charmpis DC. Seismic design optimization of multi–storey steel–concrete compo site buildings. COMPUT STRUCT 2016; 170: 49-61. https://doi.org/10.1016/j.compstruc.2016.03.010.

[4] Yu CQ, Tong GS, Tong JZ, Zhang JW, Li XG, Xu SL. Experimental and numerical study on seis mic performance of L-shaped multi-cellular CFST frames. J CONSTR STEEL RES 2024; 213: 10 8360. https://doi.org/10.1016/j.jcsr.2023.108360.

[5] Chen YL, Tong JZ, Li QH, Xu SL, Gao W, Liu X. Flexural behavior of novel profiled steel-UH TCC assembled composite bridge decks. J CONSTR STEEL RES 2024; 212: 108258. https://doi.or g/10.1016/j. jcsr.2023.108258.

[6] Xu B, Liu YJ, Zhu WQ. Comparative study on flexural behavior of steel-UHPC composite beams and steel-ordinary concrete composite beams in the negative moment zone. STRUCTURES 2023; 5 7: 105288. https://doi.org/10.1016/j.istruc.2023.105288.

[7] Pang R, Wang WJ, Zhou F, Ding SS. Experimental and analytical investigation on the compressiv e behavior of double-skin steel-concrete composite tube walls. J BUILD ENG 2023; 73: 106681. https://doi. org/10.1016/j.jobe.2023.106681.

[8] Tong JZ, Wu RM, Wang LQ. Experimental and numerical investigations on seismic behavior of st iffened corrugated steel plate shear walls. EARTHQ ENG STRUCT D 2023; 52(12): 3551-3574. ht tps://doi.org/ 10.1002/eqe.3920.

[9] Wu RM, Wang LQ, Tong JZ, Tong GS, Gao W. Elastic buckling formulas of multi-stiffened corru gated steel plate shear walls. ENG STRUCT 2024; 300: 117218. https://doi.org/10.1016/j.engstruct.2 023. 117218.

[10] Li PF, Wang HY, Nie D, Wang DY, Wang CZ. A method to analyze the long-term durability perf ormance of underground reinforced concrete culvert structures under coupled mechanical and enviro nmental loads. Journal of Intelligent Construction 2023; 1(2): 9180011https://d.oi.org/10.2 6599/JIC. 2023.9180011.

[11] Gong FY, Jacobsen S. Modeling of water transport in highly saturated concrete with wet surface d uring freeze/thaw. CEMENT CONCRETE RES 2019; 115: 294-307. https://doi.org/10.1016/j.cemcon res.201 8.08.013.

[12] Wang SQ, Xia P, Gong FY, Zeng Q, Chen KY, Zhao YX. Multi objective optimization of recycle d aggregate concrete based on explainable machine learning. J CLEAN PROD 2024; 445: 141045. https:// doi.o rg/10.1016/j.jclepro.2024.141045.
[13] Choi SW, Oh BK, Park JS, Park HS. Sustainable design model to reduce environmental impact of building construction with composite structures. J CLEAN PROD 2016; 137: 823-832. https://doi. org/10. 1016/j.jclepro.2016.07.174.
[14] Zhao H, Yang YT, Wang R, Chen WS, Wang YH, Lam D. Performance of steel–concrete compos ite walls with recycled aggregate concrete under low-velocity lateral impact loading. ENG STRUC T 2023; 296: 116899. https://doi.org/10.1016/j.engstruct.2023.116899.
[15] Wang YH, Guo LH, Li HD, Shafaei S, Yu Y. Lateral load response of L-shaped steel–concrete co mposite shear walls using multi-partition steel tube. ENG STRUCT 2023; 293: 116671. https://doi. org/10.1016/ j.engstruct.2023.116671.
[16] Ke XJ, Qin Y, Chen SJ, Li N. Seismic performance and shear lag effect of T-shaped steel plate r einforced concrete composite shear wall. ENG STRUCT 2023; 289: 116303. https://doi.org/10.1016/ j.engstruct.2 023.116303.
[17] Zhou SM, Tong JZ, Tong GS, Xu QB. Testing on global stability performance of multi-celled CF ST walls with three simply-supported edges. ENG STRUCT 2023; 291: 116478. https://doi.org/10.1 016/j.eng struct.2023.116478.
[18] Wang W, Wang Y, Lu Z. Experimental study on seismic behavior of steel plate reinforced concret e composite shear wall. ENG STRUCT 2018; 160: 281-292. https://doi.org/10.1016/j.engstruct.2018. 0105. 0.
[19] Ke XJ, Li N, Li QL, Tang ZK. Seismic behavior of steel plate concrete composite shear walls wi th PEC columns and WRGs. ENG STRUCT 2023; 277: 115412. https://doi.org/10.1016/j.engstruct.2 022.115412.
[20] Gharaei-Moghaddam N, Meghdadian M, Ghalehnovi M. Innovations and advancements in concrete-encased steel shear walls: A comprehensive review. RESULTS ENG 2023; 19: 101351. https://d oi. org/10.1016/j.rineng.2023.101351.
[21] Qin Y, Shu GP, Zhou XL, Han JH, Zhang HK. Behavior of T-shaped sandwich composite walls with truss connectors under eccentric compression. J CONSTR STEEL RES 2020; 169: 106067. ht tps://doi.o rg/10.1016/j.jcsr.2020.106067.
[22] Liu ZH, Shu GP, Luo KR, Qin Y. Performance of double-skin truss-reinforced composite wall und er axial compression. J CONSTR STEEL RES 2023; 202: 107778. https://doi.org/10.1016/j.jcsr.202 3107. 778.
[23] Nie JG, Hu HS, Fan JS, Tao MX, Li SY, Liu FJ. Experimental study on seismic behavior of hig h-strength concrete filled double-steel-plate composite walls. J CONSTR STEEL RES 2013; 88: 20 6-219. htt ps://doi.org/10.1016/j.jcsr.2013.05.001.
[24] Zhang K, Varma AH, Malushte SR, Gallocher S. Effect of shear connectors on local buckling and composite action in steel concrete composite walls. NUCL ENG DES 2014; 269: 231-239. https:/ /d oi.org/10.1016/j.nucengdes.2013.08.035.
[25] Yan JB, Wang Z, Luo YB, Wang T. Compressive behaviours of novel SCS sandwich composite w alls with normal weight concrete. THIN WALL STRUCT 2019; 141: 119-132. https://doi.org/1 0.1 016/j.tws.2019.01.051.
[26] Guo YL, Zhu JS, Wang MZ, Yang X, Zhou P. Overall instability performance of concrete-infilled double steel corrugated-plate wall. THIN WALL STRUCT 2018; 130: 372-394. https://doi.org/10.10 16/j.tw s.2018.05.026.
[27] Wang MZ, Guo YL, Yang X, Zhu JS. Compressive buckling behaviour of steel corrugated-plates i n contact with a rigid medium. COMPOS STRUCT 2021; 262: 113356. https://doi.org/10.1016/j.co mpstruc t.2020.113356.
[28] Zhu JS, Guo YL, Wang MZ, Yang X, Zhu BL. Strength design of concrete-infilled double steel c orrugated-plate walls under uniform compressions. THIN WALL STRUCT 2019; 141: 153-174. htt ps:// doi.org/10.1016/j.tws.2019.02.021.
[29] Zhang XM, Qin Y, Chen ZH. Experimental seismic behavior of innovative composite shear walls. J CONSTR STEEL RES 2016; 116: 218-232. https://doi.org/10.1016/j.jcsr.2015.09.015.
[30] Zhang XM, Qin Y, Chen ZH, Jie L. Experimental behavior of innovative T-shaped composite shea r walls under in-plane cyclic loading. J CONSTR STEEL RES 2016; 120: 143-159. https://doi.org/ 10.1016/j.jcs r.2016.01.008.
[31] Zhou SM, Tong JZ, Tong GS. Global stability tests and design of multi-celled concrete-filled steel tubular walls. J CONSTR STEEL RES 2022; 199: 107638. https://doi.org/10.1016/j.jcsr.2022.10763 8.
[32] Tong JZ, Zhang JB, Tong GS, Chen M, Zhang L, Yu CQ, Zhou SM. Flexural tests and behavior

of multi-celled corrugated-plate CFST members. J BUILD ENG 2022; 49: 104051. https://doi.org/10.101 6/j.jobe.2022.104051.
[33] Tong JZ, Yu CQ, Tong GS, Xu SL. Experimental study on axial resistant behavior of multi-celled corrugated-plate CFST walls. ENG STRUCT 2023; 295: 116795. https://doi.org/10.1016/j.engstruct.2023. 116795.
[34] Hao TY, Cao WL, Qiao QY, Liu Y, Zheng WB. Structural performance of composite shear walls under compression. Applied Sciences 2017; 7(2): 162. https://doi.org/10.3390/app7020162.
[35] Wang B, Jiang HJ, Lu XL. Seismic performance of steel plate reinforced concrete shear wall and its application in China Mainland. J CONSTR STEEL RES 2017; 131: 132-143.https://doi.org/10.1016/j.jcs r.2017.01.003.
[36] Wang JJ, Tao MX, Fan JS, Nie X. Seismic behavior of steel plate reinforced concrete composite shear walls under tension-bending-shear combined cyclic load. J STRUCT ENG 2018; 144(7). https://doi.org/1 0.1061/(ASCE)ST.1943-541X.0002073.
[37] Qi Y, Gu Q, Sun GH, Zhao BC. Shear force demand on headed stud for the design of composite steel plate shear wall. ENG STRUCT 2017; 148: 780-792. https://doi.org/10.1016/j.engstruct.2017.07.023.
[38] Lou GB, Chen PX, Zheng JH. Seismic performance of high-strength steel plate-concrete composite shear walls. J BUILD ENG 2024; 82: 108258. https://doi.org/10.1016/j.jobe.2023.108258.
[39] Xiao CZ, Zhu AP, Li JH, Li YB. Experimental study on seismic performance of embedded steel plate-HSC composite shear walls. J BUILD ENG 2021; 34: 101909. https://doi.org/10.1016/j.jobe.2020.1 01909.
[40] Jiang DQ, Xiao CZ, Chen T, Zhang YY. Experimental study of high-strength concrete-steel plate composite shear walls. Applied Sciences 2019; 9(14): 2820. https://doi.org/10.3390/app9142820.
[41] Zhang HX, Liu H, Li GC, Ning X. Seismic performance of encased steel plate-reinforced gangue concrete composite shear walls. KSCE J CIV ENG 2019; 23(7): 2919-2932. https://doi.org/10.1007/s12205-019-0286-9.
[42] Ma ZB, Wu YT, Wang X, Zhu JC. Seismic behavior of steel plate and reinforced concrete composite wall coupled to steel side columns. J BUILD ENG 2023; 65: 105820. https://doi.org/10.1016/j.jobe.2022.105 820.
[43] Dong HY, Cao WL, Wu HP, Qiao QY, Yu CP. Experimental and analytical study on seismic behavior of steel-concrete multienergy dissipation composite shear walls. EARTHQ ENG ENG VIB 2015; 14(1): 125-139. https://doi.org/10.1007/s11803-015-0011-8.
[44] Hu HS, Nie JG, Fan JS, Tao MX, Wang YH, Li SY. Seismic behavior of CFST-enhanced steel plate-reinforced concrete shear walls. J CONSTR STEEL RES 2016; 119: 176-189. https://doi.org/10.1016/j.jcsr.2015.12.010.
[45] Wang W, Ren YZ, Han B, Ren T, Liu GW, Liang YJ. Seismic performance of corrugated steel plate concrete composite shear walls. The Structural Design of Tall and Special Buildings 2019; 28 (1): https://doi.org/10.1002/tal.1564.
[46] Wang W, Ren YZ, Lu Z, Song JL, Han B, Zhou Y. Experimental study of the hysteretic behavior of corrugated steel plate shear walls and steel plate reinforced concrete composite shear walls. J CONSTR STEEL RES 2019; 160: 136-152. https://doi.org/10.1016/j.jcsr.2019.05.019.
[47] Li Y, Wang W, Su SQ, Quan CC, Jia Y, Mi JX, Xu J. Section performance analysis of vertical corrugated steel plate-reinforced concrete composite shear walls. STRUCTURES 2023; 56: 104987. https://doi.org/1 0.1016/j.istruc.2023.104987.
[48] Luo QR, Zhao SX, Wang W, Gong XB, Xia J. Research on interaction relationship and seismic performance efficiency of corrugated steel-plate composite shear wall. SOIL DYN EARTHQ ENG 2023; 172: 108046. https://doi.org/10.1016/j.soildyn.2023.108046.
[49] Song JL, Wang W, Su SQ, Ding XB, Luo QR, Quan CC. Experimental study on the bond-slip performance between concrete and a corrugated steel plate with studs. ENG STRUCT 2020; 224: 11 1195. https://doi.org/10.1016/j.engstruct.2020.111195.
[50] Wang W, Li Y, Su SQ, Quan CC, Mi JX, Xu J, Jia Y. Interfacial bonding stress transfer and failure mechanism between corrugated steel plate and reinforced concrete. ENG FAIL ANAL 2023; 153: 107555. https://doi.org/10.1016/j.engfailanal.2023.107555.
[51] Zhou Z, Qian J, Huang W. Shear strength of steel plate reinforced concrete shear wall. ADV STRUCT ENG 2020; 23(8): 1629-1643. https://doi.org/10.1177/1369433219898100.
[52] Xie QH, Xiao JZ, Xie WG, Gao WY. Cyclic tests on composite plate shear walls–concrete encased before and after fire exposure. ADV STRUCT ENG 2019; 22(1): 54-68. https://doi.org/10.1177/1369433218777837.
[53] Ren XD, Bai Q, Yang CD, Li J. Seismic behavior of tall buildings using steel–concrete composite columns and shear walls. The Structural Design of Tall and Special Buildings 2018; 27(4): https:/

/doi.org/10.1002/tal.1441.
[54] Dey S, Bhowmick AK. Seismic performance of composite plate shear walls. STRUCTURES 2016; 6: 59-72. https://doi.org/10.1016/j.istruc.2016.01.006.
[55] Wright HD, Oduyemi TOS, Evans HR. The experimental behaviour of double skin composite elem ents. J CONSTR STEEL RES 1991; 19(2): 97-110. https://doi.org/10.1016/0143-974X(91)90036-Z.
[56] Wright HD, Oduyemi TOS, Evans HR. The design of double skin composite elements. J CONST R STEEL RES 1991; 19(2): 111-132. https://doi.org/10.1016/0143-974X(91)90037-2.
[57] Link RA, Elwi AE. Composite concrete steel plate walls - analysis and behavior. J STRUCT EN G 1995; 121(2): 260-271. https://doi.org/10.1061/(ASCE)0733-9445(1995)121:2(260).
[58] Yan JB, Liew JYR, Zhang MH, Sohel KMA. Experimental and analytical study on ultimate streng th behavior of steel–concrete–steel sandwich composite beam structures. MATER STRUCT 2015; 4 8(5): 1523-1544. https://doi.org/10.1617/s11527-014-0252-4.
[59] Pryer JW, Bowerman HG. The development and use of British steel bi-steel. J CONSTR STEEL RES 1998; 46(1): 15. https://doi.org/10.1016/S0143-974X(98)00135-7.
[60] Liang QQ, Uy B, Wright HD, Bradford MA. Local Buckling of Steel Plates in Double Skin Com posite Panels under Biaxial Compression and Shear. Journal of structural engineering (New York, N.Y.) 2004; 130(3): 443-451. https://doi.org/10.1061/(ASCE)0733-9445(2004)130:3(443).
[61] Shi J, Gao S, Guo LH. Compressive behaviour of double skin composite shear walls stiffened wit h steel-bars trusses. J CONSTR STEEL RES 2021; 180: 106581. https://doi.org/10.1016/j.jcsr.2021. 106581.
[62] Eom TS, Park HG, Lee CH, Kim JH, Chang IH. Behavior of Double Skin Composite Wall Subje cted to In-Plane Cyclic Loading. Journal of structural engineering (New York, N.Y.) 2009; 135(10): 1239-1249. https://doi.org/10.1061/(ASCE)ST.1943-541X.0000057.
[63] Liew JYR, Sohel KMA, Koh CG. Impact tests on steel–concrete–steel sandwich beams with light weight concrete core. ENG STRUCT 2009; 31(9): 2045-2059. https://doi.org/10.1016/j.engstruct.200 9.03.007.
[64] Takeuchi M, Narikawa M, Matsuo I, Hara K, Usami S. Study on a concrete filled structure for n uclear power plants. NUCL ENG DES 1998; 179(2): 209-223. https://doi.org/10.1016/S0029-5493(9 7)00282-3.
[65] Yan JB, Wang XT, Wang T. Compressive behaviour of normal weight concrete confined by the st eel face plates in SCS sandwich wall. CONSTR BUILD MATER 2018; 171: 437-454. https://doi.o rg/10.1016/j.conbuildmat.2018.03.143.
[66] Yan JB, Chen A, Wang T. Axial compressive behaviours of steel–concrete-steel sandwich composit e walls with novel enhanced C-channels. STRUCTURES 2020; 28: 407-423. https://doi.org/10.1016 /j.istruc.2020.08.070.
[67] Qin Y, Shu GP, Zhou GG, Han JH. Compressive behavior of double skin composite wall with dif ferent plate thicknesses. J CONSTR STEEL RES 2019; 157: 297-313. https://doi.org/10.1016/j.jcsr.2 019.02.023.
[68] Chen ZH, Zi ZY, Zhou T, Wu YP. Axial compression stability of thin double-steel-plate and concr ete composite shear wall. STRUCTURES 2021; 34: 3866-3881. https://doi.org/10.1016/j.istruc.2021. 09.063.
[69] Yang Y, Liu JB, Fan JS. Buckling behavior of double-skin composite walls: An experimental and modeling study. J CONSTR STEEL RES 2016; 121: 126-135. https://doi.org/10.1016/j.jcsr.2016.01.0 19.
[70] Hu HS, Fang PP, Liu Y, Guo ZX, Shahrooz BM. Local buckling of steel plates in composite me mbers with tie bars under axial compression. ENG STRUCT 2020; 205: 110097. https://doi.org/10. 1016/j.engstruct.2019.110097.
[71] Harmon JR, Varma AH. Local buckling of steel faceplates anchored to concrete infill in C-PSW/C F. THIN WALL STRUCT 2021; 167: 108230. https://doi.org/10.1016/j.tws.2021.108230.
[72] Shi J, Guo LH, Gao S. Study on the buckling behavior of steel plate composite walls with diamo nd arranged studs under axial compression. J BUILD ENG 2022; 50: 104185. https://doi.org/10.10 16/j.jobe.2022.104185.
[73] Shi J, Guo LH, Gao S, Li ZG. Buckling behavior of double skin composite walls under axial co mpressive load. CONSTR BUILD MATER 2022; 321: 126345. https://doi.org/10.1016/j.conbuildmat. 2022.126345.
[74] Ozaki M, Akita S, Osuga H, Nakayama T, Adachi N. Study on steel plate reinforced concrete pa nels subjected to cyclic in-plane shear. NUCL ENG DES 2004; 228(1): 225-244. https://doi.org/10. 1016/j.nucengdes.2003.06.010.
[75] Yan JB, Li ZX, Wang T. Seismic behaviour of double skin composite shear walls with overlapped headed studs. CONSTR BUILD MATER 2018; 191: 590-607. https://doi.org/10.1016/j.conbuildmat.

2018.10.042.
[76] Shi J, Guo LH, Qu B. In-plane cyclic tests of double-skin composite walls with concrete-filled ste el tube boundary elements. ENG STRUCT 2022; 250: 113301. https://doi.org/10.1016/j.engstruct.20 21.113301.
[77] Long Z, Zhong M. Experimental study on the vertical temperature and thermal stratification for su bway station fire. Journal of Intelligent Construction 2023; 1(4): 9180030. https://doi.org/10.26599/J IC.2023.9180030.
[78] Wei F, Fang C, Wu B. Fire resistance of concrete-filled steel plate composite (CFSPC) walls. FIR E SAFETY J 2017; 88: 26-39. https://doi.org/10.1016/j.firesaf.2016.12.008.
[79] Taghipour Anvari A, Bhardwaj SR, Sharma S, Varma AH. Performance of Composite Plate Shear Walls/Concrete Filled (C-PSW/CF) Under Fire Loading: A Numerical Investigation. ENG STRUCT 2022; 271: 114883. https://doi.org/10.1016/j.engstruct.2022.114883.
[80] Hu B, Huang JQ, Lou GB. Degradation of Out-of-plane Initial Stiffness of Steel-concrete Walls E xposed to Fire. INT J STEEL STRUCT 2018; 18(1): 51-67. https://doi.org/10.1007/s13296-018-030 5-6.
[81] Du EF, Shu GP, Qin L, Lai BL, Zhou XL, Zhou GG. Experimental investigation on fire resistanc e of sandwich composite walls with truss connectors. J CONSTR STEEL RES 2022; 188: 107052. https://doi.org/10.1016/j.jcsr.2021.107052.
[82] McKinley B, Boswell LF. Behaviour of double skin composite construction. J CONSTR STEEL R ES 2002; 58(10): 1347-1359. https://doi.org/10.1016/S0143-974X(02)00015-9.
[83] Sener KC, Varma AH. Steel-plate composite walls: Experimental database and design for out-of-pl ane shear. J CONSTR STEEL RES 2014; 100: 197-210. https://doi.org/10.1016/j.jcsr.2014.04.014.
[84] Sener KC, Varma AH, Ayhan D. Steel-plate composite (SC) walls: Out-of-plane flexural behavior, database, and design. J CONSTR STEEL RES 2015; 108: 46-59. https://doi.org/10.1016/j.jcsr.2015. 02.002.
[85] Varma AH, Malushte SR, Sener KC, Lai ZC. Steel-plate composite (SC) walls for safety related n uclear facilities: Design for in-plane forces and out-of-plane moments. NUCL ENG DES 2014; 26 9: 240-249. https://doi.org/10.1016/j.nucengdes.2013.09.019.
[86] Yang Y, Wu B, Xu LY, Yao YP, Zhang D, Zhao C. Experimental study on the buckling behavior of double steel plate concrete composite slabs with stiffening ribs and tie plates. ENG STRUCT 2 022; 255: 113895. https://doi.org/10.1016/j.engstruct.2022.113895.
[87] Wright HD, Evans HR, Harding PW. The use of profiled steel sheeting in floor construction. J C ONSTR STEEL RES 1987; 7(4): 279-295. https://doi.org/10.1016/0143-974X(87)90003-4.
[88] Wright HD. The axial load behaviour of composite walling. J CONSTR STEEL RES 1998; 45 (3): 353-375. https://doi.org/10.1016/S0143-974X(97)00030-8.
[89] Hossain KMA, Mol LK, Anwar MS. Axial load behaviour of pierced profiled composite walls wit h strength enhancement devices. J CONSTR STEEL RES 2015; 110: 48-64. https://doi.org/10.1016/ j.jcsr.2015.03.009.
[90] Uy B, Wright HD, Bradford MA. Combined axial and flexural strength of profiled composite wall s. P I CIVIL ENG-STR B 2001; 146(2): 129-139. https://doi.org/10.1680/stbu.2001.146.2.129.
[91] Tong JZ, Pan WH, Shen MH. Performance of double-skin composite walls with re-entrant profiled faceplates under eccentric compression. J BUILD ENG 2020; 28: 101010. https://doi.org/10.1016/j. jobe.2019.101010.
[92] Tong JZ, Yu CQ, Zhang L. Sectional strength and design of double-skin composite walls withre-e ntrant profiled faceplates. THIN WALL STRUCT 2021; 158: 107196. https://doi.org/10.1016/j.tws.2 020.107196.
[93] Zhou YQ, Zhu JS, Guo YL, Wang MZ, Yang X, Ren YH. Numerical and experimental studies on sectional load capacity of concrete-infilled double steel corrugated-plate walls under combined co mpression and in-plane bending. THIN WALL STRUCT 2021; 159: 107250. https://doi.org/10.1016/ j.tws.2020.107250.
[94] Wang MZ, Guo YL, Zhu JS, Yang X, Tong JZ. Sectional strength design of concrete-infilled doub le steel corrugated-plate walls with T-section. J CONSTR STEEL RES 2019; 160: 23-44. https://do i.org/10.1016/j.jcsr.2019.05.017.
[95] Wang MZ, Guo YL, Zhu JS, Yang X. Flexural buckling of axially loaded concrete-infilled double steel corrugated-plate walls with T-section. J CONSTR STEEL RES 2020; 166: 105940. https://doi. org/10.1016/j.jcsr.2020.105940.
[96] Wang MZ, Guo YL, Zhu JS, Yang X. Flexural-torsional buckling and design recommendations of axially loaded concrete-infilled double steel corrugated-plate walls with T-section. ENG STRUCT 2 020; 208: 110345. https://doi.org/10.1016/j.engstruct.2020.110345.
[97] Wang MZ, Guo YL, Yang X, Zhu JS. Interaction equations of composite walls with T-section und

er axial compression and biaxial bending. ENG STRUCT 2021; 229: 111667. https://doi.org/10.1016/j.engstruct.2020.111667.
[98] Hossain KMA, Wright HD. Performance of profiled concrete shear panels. J STRUCT ENG 1998; 124 (4): 368-381. https://doi.org/10.1061/(ASCE)0733-9445(1998)124:4(368).
[99] Hossain KMA, Wright HD. Performance of double skin-profiled composite shear walls experiments and design equations. CAN J CIVIL ENG 2004; 31(2): 204-217. https://doi.org/10.1139/l03-087.
[100] Hossain KMA, Wright HD. Experimental and theoretical behaviour of composite walling under in-plane shear. J CONSTR STEEL RES 2004; 60(1): 59-83. https://doi.org/10.1016/j.jcsr.2003.08.004.
[101] Rafiei S, Hossain KMA, Lachemi M, Behdinan K, Anwar MS. Finite element modeling of double skin profiled composite shear wall system under in-plane loadings. ENG STRUCT 2013; 56: 46-57. https://doi.org/10.1016/j.engstruct.2013.04.014.
[102] Rafiei S, Hossain KMA, Lachemi M, Behdinan K. Profiled sandwich composite wall with high performance concrete subjected to monotonic shear. J CONSTR STEEL RES 2015; 107: 124-136. https://doi.org/10.1016/j.jcsr.2015.01.015.
[103] Zhou J, Chen ZP, Liao HY, Tang JY. Seismic behavior of corrugated double-skin composite wall (DSCW) with concrete-filled steel tubes: Experimental investigation. ENG STRUCT 2022; 252: 113632. https://doi.org/10.1016/j.engstruct.2021.113632.
[104] Hossain KMA, Rafiei S, Lachemi M, Behdinan K. Structural performance of profiled composite wall under in-plane cyclic loading. ENG STRUCT 2016; 110: 88-104. https://doi.org/10.1016/j.engstruct.2015.11.057.
[105] Zhao QH, Li YK, Tian Y. Cyclic behavior of double-skin composite walls with flat and corrugated faceplates. ENG STRUCT 2020; 220: 111013. https://doi.org/10.1016/j.engstruct.2020.111013.
[106] Zhu JS, Guo YL, Wang MZ, Yang X, Pi YL. Seismic performance of concrete-infilled double steel corrugated-plate walls: Experimental research. ENG STRUCT 2020; 215: 110601. https://doi.org/10.1016/j.engstruct.2020.110601.
[107] Le QX, Dao VTN, Torero JL, Ngo TD. Experimental study into the behaviour of profiled composite walls under combined axial and thermal loadings. ENG STRUCT 2020; 210: 110354. https://doi.org/10.1016/j.engstruct.2020.110354.
[108] Le QX, Dao VTN, Torero JL. Understanding the performance of profiled composite walls in fire. ENG STRUCT 2023; 282: 115790. https://doi.org/10.1016/j.engstruct.2023.115790.
[109] Rafiei S, Hossain KMA, Lachemi M, Behdinan K. Impact shear resistance of double skin profiled composite wall. ENG STRUCT 2017; 140: 267-285. https://doi.org/10.1016/j.engstruct.2017.02.062.
[110] Link RA, Elwi AE. Composite concrete steel plate walls - analysis and behavior. J STRUCT ENG 1995; 121(2): 260-271. https://doi.org/10.1061/(ASCE)0733-9445(1995)121:2(260).
[111] Guo LH, Wang YH, Zhang SM. Experimental study of rectangular multi-partition steel-concrete composite shear walls. THIN WALL STRUCT 2018; 130: 577-592. https://doi.org/10.1016/j.tws.2018.06.011.
[112] Li HB, Yan PF, Sun H, Yin JG. Axial compression performance and ultrasonic testing of multicavity concrete-filled steel tube shear wall under axial load. ADV CIV ENG 2020; 2020: 1-19. https://doi.org/10.1155/2020/8877282.
[113] Zhang YJ, Tong GS, Tong JZ, Zhou Y, Zhang L, Yu CQ. Experimental and numerical study on post-ultimate ductile performance of multi-celled concrete-filled steel tubular walls. J CONSTR STEEL RES 2023; 211: 108097. https://doi.org/10.1016/j.jcsr.2023.108097.
[114] Wang SY, Wang W, Xie SW, Chen YS. Behavior and design method of double skin composite wall under axial compression. J BUILD ENG 2023; 64: 105554. https://doi.org/10.1016/j.jobe.2022.105554.
[115] Zhou SM, Tong JZ, Tong GS. Global buckling design of multi-celled CFST walls with four simply-supported edges. THIN WALL STRUCT 2021; 165: 107966. https://doi.org/10.1016/j.tws.2021.107966.
[116] Zhou SM, Tong JZ, Tong GS. Determining experimental ductile behavior of composite walls considering second-order effects: A case study for multi-celled CFST walls. STRUCTURES 2023; 57: 105121. https://doi.org/10.1016/j.istruc.2023.105121.
[117] Huang ST, Huang YS, He A, Tang XL, Chen QJ, Liu XP, Cai J. Experimental study on seismic behaviour of an innovative composite shear wall. J CONSTR STEEL RES 2018; 148: 165-179. https://doi.org/10.1016/j.jcsr.2018.05.003.
[118] Tong GS, Lin CH, Hu ZZ, Yang SL. Experimental study on seismic behavior of innovative multi-cellular CFT-walls with tie-bolts. ADV STEEL CONSTR 2021; 17(1): 39-49. https://doi.org/10.18057/IJASC.2021.17.1.5.
[119] Li J, Wang Z, Li F, Mou B, Wang T. Experimental and numerical study on the seismic performance of an L-shaped double-steel plate composite shear wall. J BUILD ENG 2022; 49: 104015. htt

ps://doi.org/10.1016/j.jobe.2022.104015.
[120] Chen LH, Wang SY, Lou Y, Xia DR. Seismic behavior of double-skin composite wall with L-sha ped and C-shaped connectors. J CONSTR STEEL RES 2019; 160: 255-270. https://doi.org/10.1016/ j.jcsr.2019.05.033.
[121] Chen LH, Yin C, Wang CG, Liu YM. Experimental study on seismic behavior of double-skin co mposite wall with L-shaped connectors. J CONSTR STEEL RES 2020; 174: 106312. https://doi.org /10.1016/j.jcsr.2020.106312.
[122] Chen LH, Bai S, Zhou LJ, Zhou A. Experimental study and numerical simulation on seismic beha vior of double-skin composite wall. J CONSTR STEEL RES 2021; 187: 106935. https://doi.org/10. 1016/j.jcsr.2021.106935.
[123] Wang SY, Wang W, Chen YS, Hou HW, Xie SW. Seismic performance of double skin composite wall under maximum considered far-field earthquake loading protocol. J BUILD ENG 2022; 55: 1 04705. https://doi.org/10.1016/j.jobe.2022.104705.
[124] Wang SY, Wang W. Development of loading protocols for experimental testing of double skin co mposite wall. J BUILD ENG 2022; 51: 104324. https://doi.org/10.1016/j.jobe.2022.104324.
[125] Liu JQ, Han LH, Zhao XL. Performance of concrete-filled steel tubular column-wall structure subj ected to ISO-834 standard fire: analytical behaviour. THIN WALL STRUCT 2018; 129: 28-44. htt ps://doi.org/10.1016/j.tws.2018.03.027.
[126] Liu JQ, Han LH, Zhao XL. Performance of concrete-filled steel tubular column-wall structure subj ected to ISO-834 standard fire: Experimental study and FEA modelling. THIN WALL STRUCT 20 17; 120: 479-494. https://doi.org/10.1016/j.tws.2017.09.014.
[127] Tong GS, Zhou SM, Tong JZ, Zhang L, Yu CQ. Experimental study on tensile fracture mechanis m of butt joints in multi-celled CFST walls. J BUILD ENG 2022; 52: 104422. https://doi.org/10.1 016/j.jobe.2022.104422.
[128] Tong GS, Hu ZZ, Chen Y. Study on the moment capacity of a connection joining an I-beam to c oncrete-filled multicellular steel tube walls. J CONSTR STEEL RES 2021; 182: 106643. https://do i.org/10.1016/j.jcsr.2021.106643.
[129] Guo LH, Gao S, Mu CM. Behaviour of MCFST column-steel beam connection with side plates in the scenario of column loss. J CONSTR STEEL RES 2020; 171: 106150. https://doi.org/10.1016/j. jcsr.2020.106150.
[130] An Q, Wang Y, Yu HR, Wang XJ. Seismic behaviour of anchored prefabricated wall–beam joints of bundled lipped channel-concrete composite wall structures. THIN WALL STRUCT 2022; 179: 1 09695. https://doi.org/10.1016/j.tws.2022.109695.
[131] Xu D, Xiang BQ, Chong X, Xu KY, Yan JB, Wang T. Seismic performances of the joint between replaceable-coupling beams and composite shear wall. J CONSTR STEEL RES 2022; 197: 10746 2. https://doi.org/10.1016/j.jcsr.2022.107462.
[132] Yu CQ, Tong JZ, Tong GS, Xu SL, Chen M. Axial compressive performance and design of multi -celled corrugated-plate CFST walls. STRUCTURES 2023; 57: 105303. https://doi.org/10.1016/j.istru c.2023.105303.
[133] Tong JZ, Yu CQ, Tong GS, Chen M, Zhang L. Stability behavior of multi-celled corrugated-plate concrete filled steel tubular walls. Journal of Building Structures 2023; 44(5): 240-251,285. (in Chi nese) https://doi.org/10.14006/j.jzjgxb.2021.0834.
[134] Li X, Liao X, Li ZY, Song DY, Yin DD. Confinement mechanism of rectangular CFST componen ts using double horizontally-corrugated steel plates. STRUCTURES 2023; 57: 105107. https://doi.or g/10.1016/j.istruc.2023.105107.
[135] Zhang JW, Tong JZ, Yu CQ, Tong GS, Chen M, Zhang L, Yang SL. Experimental evaluation on seismic performance of multi-celled corrugated-plate CFST walls. J CONSTR STEEL RES 2023; 2 01: 107743. https://doi.org/10.1016/j.jcsr.2022.107743.
[136] Tong JZ, Zhang JM, Yu CQ, Tong GS, Li QH, Xu SL. Seismic experiments and shear resistance prediction of multi-celled corrugated-plate CFST walls. EARTHQ ENG STRUCT D 2024; 53(5): 1 681-1704. https://doi.org/10.1002/eqe.4091.
[137] Duan SJ, Tong GS, Tong JZ. Behavior and design of steel beam to multi-celled corrugated-plate CFST wall joints. J CONSTR STEEL RES 2024; 214: 108468. https://doi.org/10.1016/j.jcsr.2024.10 8468.
[138] JGJ 138, Code for design of composite structures[S]. Beijing: China Architecture & Building Pres s, 2016. (in Chinese).
[139] Luo QR, Wang W, Sun ZZ, Xu SW, Wang BJ. Seismic performance analysis of corrugated-steel-pl ate composite shear wall based on corner failure. J CONSTR STEEL RES 2021; 180: 106606. htt ps://doi.org/10.1016/j.jcsr.2021.106606.
[140] AIJ, Recommendations for design and construction of concrete filled steel tubular structures[S]. To

kyo: Architectural Institute of Japan, 2008.
[141] AISC 360, Specification for structural steel buildings[S]. Chicago: American Institute of Steel Construction, 2022.
[142] BS 5400, Steel, concrete and composite bridges: Part 5: Code of practice for design of composite bridges[S]. British: British Standards Institution, 2005.
[143] EC4, Eurocode 4: Design of composite steel and concrete structures—Part 1-1: General rules and rules for buildings[S]. Brussels: European Committee for Standardization, 2004.
[144] Mander JB, Priestley MJN, Park R. Theoretical stress-strain model for confined concrete. J STRUCT ENG 1988; 114 (8): 1804-1826. https://doi.org/10.1061/(ASCE)0733-9445(1988)114:8(1804).
[145] Hou HW, Wang W, Wang SY. Nonlinear modeling methods for cyclic analysis of double-skin composite shear walls. THIN WALL STRUCT 2023; 187: 110737. https://doi.org/10.1016/j.tws.2023.110737.
[146] Liu ZH, Shu GP, Zhu H, Qin Y. Behavior of double-skin truss-reinforced composite walls under eccentric compression. STRUCTURES 2023; 51: 718-733. https://doi.org/10.1016/j.istruc.2023.03.068.
[147] Xiong MX, Xiong DX, Liew JYR. Axial performance of short concrete filled steel tubes with high- and ultra-high- strength materials. ENG STRUCT 2017; 136: 494-510. https://doi.org/10.1016/j.engstruct.2017.01.037.
[148] Chen YL, Tong JZ, Li QH, Xu SL, Shen LM. Application of high-performance cementitious composites in steel–concrete composite bridge deck systems: A review. Journal of Intelligent Construction 2024: https://doi.org/10.26599/JIC.2024.9180012.
[149] Zhi D, Xia P, Wang SQ, Gong FY, Cao WL, Wang DM, Ueda T. RBSM-based mesoscale study of mechanical properties and frost damage behaviors for recycled fine aggregate concrete. CONSTR BUILD MATER 2024; 416: 135136. https://doi.org/10.1016/j.conbuildmat.2024.135136.
[150] Xia P, Wang SQ, Gong FY, Cao WL, Zhao YX. Rapid recognition method of red brick content in recycled brick-concrete aggregates and powder based on color segmentation. J BUILD ENG 2024; 84: 108633. https://doi.org/10.1016/j.jobe.2024.108633.
[151] Xia P, Wang SQ, Chen KY, Meng T, Chen XD, Gong FY. A recycling approach of natural stone from crushed concrete based on freeze-thaw modification and usage of spalling mortar as recycled fine aggregate. CONSTR BUILD MATER 2024; 416: 135287. https://doi.org/10.1016/j.conbuildmat.2024.135287.